The $X\,^1\Sigma_g^+$, $B\,^1\Delta_g$, and $B'\,^1\Sigma_g^+$ states of C$_2$: A comparison of renormalized coupled-cluster and multireference methods with full configuration interaction benchmarks

C. David Sherrill[a)]
Center for Computational Molecular Science and Technology, School of Chemistry and Biochemistry, Georgia Institute of Technology, Atlanta, Georgia 30332-0400

Piotr Piecuch[b)]
Department of Chemistry and Department of Physics and Astronomy, Michigan State University, East Lansing, Michigan 48824

Unusual bonding and electronic near degeneracies make the lowest-lying singlet states of the C$_2$ molecule particularly challenging for electronic structure theory. Here we compare two alternative approaches to modeling bond-breaking reactions and excited states: sophisticated multireference configuration interaction and multireference perturbation theory methods, and a more "black box," single-reference approach, the completely renormalized coupled-cluster method. These approximate methods are assessed in light of their ability to reproduce the full configuration interaction potential energy curves for the $X\,^1\Sigma_g^+$, $B\,^1\Delta_g$, and $B'\,^1\Sigma_g^+$ states of C$_2$, which are numerically exact solutions of the electronic Schrödinger equation within the space spanned by a 6-31G* basis set. Both the multireference methods and the completely renormalized coupled-cluster approach provide dramatic improvements over the standard single-reference methods. The multireference methods are nearly as reliable for this challenging test case as for simpler reactions which break only single bonds. The completely renormalized coupled-cluster approach has difficulty for large internuclear separations R in this case, but over the wide range of $R=1.0–2.0$ Å, it compares favorably with the more complicated multireference methods. © *2005 American Institute of Physics.*
[DOI: 10.1063/1.1867379]

I. INTRODUCTION

The C$_2$ molecule is central to interstellar chemistry and combustion reactions. It features many low-lying electronic excited states, the first one being a $^3\Pi_u$ state only 716 cm^{-1} above the $X\,^1\Sigma_g^+$ ground state. These electronic near degeneracies are challenging for experiment and theory. Experimentally, there was some early confusion about the correct ground state of C$_2$, with Herzberg[1] listing it as the $^3\Pi_u$ state rather than $^1\Sigma_g^+$ (this was corrected later in Huber and Herzberg[2]). Theoretically, electronic near degeneracies in C$_2$ are quite significant even near the equilibrium geometry, causing difficulties for the most commonly used "single-reference" methods which rely upon the dominance of a single Hartree–Fock determinant. Stretched geometries increase the degree of electronic degeneracy and become even more problematic. For these reasons, C$_2$ makes an excellent test case to assess the robustness of theoretical methods in applications involving quasidegenerate ground and excited states, and potential energy surfaces involving bond breaking.

In a recent paper,[3] we presented full configuration interaction (full CI) potential energy curves for the $X\,^1\Sigma_g^+$, $B\,^1\Delta_g$, and $B'\,^1\Sigma_g^+$ states of C$_2$. By definition, a full CI wave func-

tion includes all possible Slater determinants (or configuration state functions) which can be formed for the given number of electrons and orbitals (and which have the appropriate symmetry). Thus, the full CI method provides an exact treatment of electron correlation within the space spanned by the given one-electron basis set, and full CI results are critical as benchmarks against which approximate methods may be assessed. The availability of full CI results is particularly useful for calculations involving ground- and excited-state potential energy surfaces along bond-breaking coordinates, where electron correlation effects become large and rapidly changing with the nuclear geometry, causing severe difficulties for the majority of electronic structure methods.

It is well known that the restricted Hartree–Fock (RHF) method fails qualitatively for bond-breaking reactions. Unrestricted Hartree–Fock (UHF) reference functions provide considerably better energies, but they are usually quantitatively poor and the wave functions are no longer eigenfunctions of $\hat{S}^2$. In some cases, such as the well-known example of the F$_2$ molecule, UHF fails in a quantitative and qualitative sense, providing a potential curve with no minimum on it (cf., e.g., Ref. 4). The deficiencies of the RHF, UHF, and other independent-particle-model approximations employing single-determinantal wave functions are often so severe that they cannot be eliminated by the addition of electron correlation via the usual single-reference methods. This, in particular, applies to the otherwise successful methods based on

---
[a)]Author to whom correspondence should be addressed. Electronic mail: sherrill@chemistry.gatech.edu
[b)]Electronic mail: piecuch@cem.msu.edu

coupled-cluster (CC) theory.[5] The RHF-based CC approximations, including the basic CCSD (CC singles and doubles) approach,[6–10] and the popular noniterative triples approaches of the CCSD[T] (Refs. 11 and 12) or CCSD(T) (Ref. 13) type, in which the effects of triply and other higher-than-doubly excited clusters are estimated using the arguments originating from many-body perturbation theory, completely fail in the bond breaking region (cf., e.g., Refs. 3, 4, and 14–30 for examples). In the case of multiple bond dissociations (including C_2), even the full CCSDT (CC singles, doubles, and triples) method[31,32] and the noniterative treatments of quadruply excited clusters via, for example, the $CCSD(TQ_f)$ approach[33] are not powerful enough to overcome the failures of the CCSD and CCSD(T) schemes.[20,22,24,25,27,28] Similar failures are observed in the calculations of excited states employing the response CC (Refs. 34–39) and equation-of-motion CC (EOMCC) (Refs. 40–43) theories. The standard response CC and EOMCC methods, including the basic EOMCCSD approximation[40–42] and its EOMCCSDT-n,[44,45] CC3,[46–49] EOMCCSD(T),[44] EOMCCSD($\tilde{T}$),[45] EOMCCSD(T′),[45] and CCSDR(3) (Refs. 48 and 49) extensions, in which the effects of triple excitations are estimated using the arguments originating from perturbation theory, fail to describe excited states having large contributions due to doubly excited configurations and excited-state potential energy surfaces along bond breaking coordinates.[24,25,28,42,44–59] The high-level EOMCC approximations, such as EOMCCSDT (the EOMCC singles, doubles, and triples method[54,55]) (cf. also Ref. 60) and EOMCCSDTQ (the EOMCC singles, doubles, triples, and quadruples method[61]) eliminate these failures, although the EOMCCSDT approach can only partly reduce large errors in the vertical excitation energies obtained in the EOMCCSD, EOMCCSDT-n, and CC3 calculations for the $B\ ^1\Delta_g$ state of C_2, leaving the 0.41 eV difference with the full CI result unaccounted for[25,28,54] (one has to use the full EOMCCSDTQ method to reduce this error to 0.02 eV).[61] Based on the early positive experiences with the UHF-based CC methods (cf., e.g., Refs. 4 and 62), it is often assumed that the use of the UHF rather than RHF reference functions should automatically eliminate the failures observed in the standard RHF-based CC calculations, but there is a growing evidence that one has to be very careful about employing UHF references in correlated calculations, since the results are often much worse than expected (cf., e.g., Refs. 63 and 64). For example, in a recent full CI study[30] of "easy" bond-breaking reactions which remove a hydrogen atom from BH, CH_4, and HF, we found surprisingly large nonparallelity errors (NPEs; NPE is defined as the difference between the maximum and minimum errors along a potential energy curve) even for highly correlated methods employing UHF determinants as references. For the UHF-based CCSD(T) approach [UHF CCSD(T)], NPEs were around 4 kcal mol^{-1}, which is more than one might expect in such simple cases. For the more challenging case of C_2, the performance of UHF-based single-reference methods was much worse.[3] UHF CCSD(T) gave a NPE of more than 20 kcal mol^{-1} for the ground state. This is better than the NPE of over 60 kcal mol^{-1} observed in the RHF-based CCSD(T) calculations, but clearly the large

NPE of more than 20 kcal mol^{-1} contradicts the common wisdom that the UHF-based approaches are panacea for the failures of single-reference methods employing the RHF reference. Based on the earlier experiences with EOMCC methods,[24,25,28,54–59] it is not surprising that the RHF-based EOMCCSD approach cannot give reasonable results for the potential energy curves corresponding to the $B\ ^1\Delta_g$ and $B'\ ^1\Sigma_g^+$ excited states of C_2, although, as shown in Ref. 3 and as further elaborated on in this paper, the failure of the EOMCCSD method for the potential curves of the $B\ ^1\Delta_g$ and $B'\ ^1\Sigma_g^+$ states of C_2 is more dramatic than in other cases. Surprisingly enough, the expensive high-level single-reference CI calculations, such as CISDTQ (CI singles, doubles, triples, and quadruples), which often provide a virtually exact and well-balanced description of ground and excited states, fail too, providing NPEs on the order of 23–24 kcal mol^{-1} for the $B\ ^1\Delta_g$ and $B'\ ^1\Sigma_g^+$ states of C_2.[3]

The low-lying states of C_2 are so challenging and the failures of various high-level electronic structure methods are so dramatic that it is desirable to use the full CI results obtained in Ref. 3 to assess the reliability of methods which are designed to handle bond breaking, excited states, and electronic near degeneracies or to improve single-reference results in all of these situations. Specifically, in this paper, we consider multireference configuration interaction (MRCI), multireference perturbation theory (MRPT), and the completely renormalized (CR) CC[18–29,58] and EOMCC (Refs. 25, 28, and 58) methods. MRCI is perhaps the most widely applicable and commonly used method for modeling bond-breaking reactions and ground- and excited-state potential energy surfaces in small molecules; if properly used, it can give very reliable results across an entire potential energy surface. Its principal shortcomings are lack of size extensivity (the fraction of the correlation energy recovered decreases for larger molecules), its great computational cost, and the requirement that the user must specify several parameters such as active orbitals, reference determinants, or thresholds for neglecting unimportant electron configurations. At present, a universally applicable and accepted methodology for choosing these parameters is absent.[65,66] The MRPT methods, such as the popular complete-active-space second-order perturbation theory (CASPT2) model[67–70] and its variants[71–79] (cf. Ref. 80 for a review), offer an alternative, less expensive, approach. However, like MRCI, CASPT2 and other multireference perturbation theory models are difficult to use for nonexperts. They can also be prohibitively expensive if the numbers of active electrons and orbitals become large. In addition, some MRPT methods may suffer from intruder states and a strong dependence of the results on the choice of active space (cf., e.g., Ref. 80). Nevertheless, both MRCI and CASPT2 approaches are specifically designed to describe bond breaking and quasidegenerate ground and excited states. Thus, it is useful to test the performance of these most popular multireference methods in a demanding situation created by ground and excited states of the C_2 molecule.

In contrast to multireference approaches, the CR-CC and CR-EOMCC methods, such as CR-CCSD(T), CR-CCSD(TQ),[18–21,23–29,58] and CR-EOMCCSD(T),[25,28,58]

are built upon a single-reference CC/EOMCC framework, and as such are "black-box" methods that are no more difficult to use than the standard noniterative CC approaches of the CCSD(T) or CCSD(TQ$_f$) type. These methods are based on the more general formalism of the method of moments of CC equations (the MMCC formalism),[18,19,25,28,56,57] which provides detailed information about the many-body structure of the differences between the CC or EOMCC and full CI energies of the electronic states of interest. This information enables one to suggest several types of the *a posteriori* noniterative corrections due to triples or triples and quadruples to standard CCSD or EOMCCSD energies, defining the CR-CCSD(T), CR-CCSD(TQ), and CR-EOMCCSD(T) approximations, which have the same computer costs as the standard triples and quadruples corrections defining the CCSD(T) and CCSD(TQ$_f$) approaches and which improve the results of single-reference CC/EOMCC calculations for quasidegenerate ground and excited states characterized by large nondynamical correlation effects. Previous experience indicates that CR-CCSD(T), CR-CCSD(TQ), and CR-EOMCCSD(T) approaches can be quite successful in describing bond breaking,[18–21,23–25,27,28,58] exchange chemical reactions,[25–29] diradicals,[81–83] excited states dominated by doubles,[25,28,58] and at least some excited-state potential energy surfaces along bond-breaking coordinates.[28,58] However, these methods have never been thoroughly tested in the most challenging environment of configurational quasidegeneracies combined with curve crossings and avoided crossings created by the $X\,{}^1\Sigma_g^+$, $B\,{}^1\Delta_g$, and $B'\,{}^1\Sigma_g^+$ states of C_2. In this case, the CCSD and EOMCCSD wave functions, on which the CR-CCSD(T), CR-CCSD(TQ), and CR-EOMCCSD(T) approaches are based, are not only quantitatively, but also qualitatively incorrect and this may severely impact the CR-CCSD(T), CR-CCSD(TQ), and CR-EOMCCSD(T) results. Although one should not expect the relatively inexpensive single-reference, RHF-based CR-CCSD(T), CR-CCSD(TQ), and CR-EOMCCSD(T) methods to perform as well as the best CASSCF-based (CASSCF—complete-active-space self-consistent-field) multireference approaches, it is interesting to learn how much information about ground- and excited-state potential curves of the difficult C_2 system can be extracted from these inexpensive black-box calculations. There exist several alternatives to the CR-CC and CR-EOMCC approaches, which are formulated in a single-reference framework and which can be applied to certain classes of bond-breaking reactions and quasidegeneracies,[14,16,17,21,84–101] and excited-state potential energy surfaces along bond-breaking coordinates,[53–55] but examination of all of these methods lies beyond the scope of the present work.

Prior to our recent 6-31G* full CI benchmark study,[3] potential curves for C_2 had been examined using a smaller basis[24,25] or at a limited number of geometries.[102] The authors of Refs. 24 and 25 compared the full CI potential curves obtained with the double ζ (DZ) basis set with the corresponding CR-CCSD(T) and CR-CCSD(TQ) curves, but at that time the 6-31G* full CI results were not available, so it was not possible to test the CR-CCSD(T) and CR-CCSD(TQ) methods in more realistic calculations employing a basis set of the DZ plus polarization (DZP) quality. More-

over, the CR-CCSD(T), CR-CCSD(TQ), and full CI calculations reported in Refs. 24 and 25 were limited to the $X\,{}^1\Sigma_g^+$ state only. Full CI vertical excitation energies have been reported in Ref. 49 and full CI spectroscopic constants have been obtained in Refs. 103 and 104. In particular, the authors of Ref. 49 have used their full CI data to assess the performance of the standard EOMCC/response CC methods, such as EOMCCSD and CC3, in calculations of vertical excitation energies of C_2. These studies have been extended by the authors of Refs. 25 and 54, who demonstrated, for example, that the failure of the standard EOMCCSD and CC3 approaches to describe vertical excitation energy corresponding to the $X\,{}^1\Sigma_g^+ \rightarrow B\,{}^1\Delta_g$ transition can be considerably reduced by employing the full EOMCCSDT theory and its active-space EOMCCSDt variant (see Ref. 61 for the most recent full EOMCCSDTQ calculations). The full CI results reported in Ref. 49 have also been used to test the performance of the CR-EOMCCSD(T) (Refs. 28 and 58) and other excited-state MMCC (Refs. 25, 28, and 57) approximations. These studies have shown that the CR-EOMCCSD(T) and other MMCC methods are capable of reducing large, >1 eV, errors in vertical excitation energies obtained with the EOMCCSD method to ~0.1 eV, but neither the CR-EOMCCSD(T) method nor any other MMCC approximation has been used to examine the entire potential energy curves of the excited states of C_2. Again, this was not possible until now because of the lack of the corresponding full CI data, which were published only recently.[3] This paper reports the CR-CC and CR-EOMCC studies of the ground- and excited-state potential curves of C_2 for the first time.

Finally, we should mention that high-quality computations of the 12 lowest singlet and triplet electronic states of C_2 have been obtained by Halvick and co-workers[105] using contracted MRCI wave functions and a large cc-pV5Z basis set. These results should be very reliable, but it is not possible to obtain full CI energies with the cc-pV5Z basis for comparison. Here, direct comparison to full CI results in the 6-31G* basis allows us to carefully examine the accuracy of MRCI, CASPT2, and CR-CC/CR-EOMCC methods for the entire potential energy curves of the $X\,{}^1\Sigma_g^+$, $B\,{}^1\Delta_g$, and $B'\,{}^1\Sigma_g^+$ states, all of which have a strong multireference character.

II. THEORETICAL APPROACH

As in our recent full CI benchmark study,[3] we have used the 6-31G* basis set. Perhaps surprisingly, this basis gives better spectroscopic constants on average (as compared to experiment) than other basis sets of DZP quality for full CI wave functions.[104] All six Cartesian d-type polarization functions were used and the lowest two (core-type) orbitals were kept frozen in all correlated calculations.

We begin the discussion of methods used in this study with details of multireference calculations. To account for near-degeneracies of electron configurations, we have used CASSCF (Ref. 106) reference wave functions, which include all configurations which can be generated by distributing the active electrons among the active orbitals. For this case, we have chosen all valence electrons and orbitals as active; this

yields a CASSCF wave function comprising 660 $M_s=0$ determinants of A_g symmetry in the D_{2h} computational subgroup. The CASSCF wave function should provide a reasonable zero-order description for any of the three valence states considered here. We also considered the possibility of a smaller active space, but the full CI results indicate that almost all of the valence orbitals have variable occupations among the most important electron configurations. Limited computations were also performed in which the $2\sigma_g$ orbital, which is usually doubly occupied, was left out of the active space.

Although there is no difficulty obtaining the CASSCF wave function for the lowest $^1\Sigma_g^+$ state, it is technically challenging to obtain a CASSCF solution for the higher $^1\Sigma_g^+$ state. One could optimize orbitals for the second root of this symmetry in the CASSCF wave function, but eventually this root can be improved to the point that it drops below the lower $^1\Sigma_g^+$ state, leading to "root flipping" and convergence difficulties. This problem may be circumvented by using "state averaged" (SA) orbitals[107,108] obtained by varying orbitals to minimize the weighted sum of the CASSCF energies for the two $^1\Sigma_g^+$ states. We have used SA orbitals to obtain CASSCF energies for the two $^1\Sigma_g^+$ states (each state is equally weighted).

The $^1\Delta_g$ state has the same symmetry as the $^1\Sigma_g^+$ states in the D_{2h} computational subgroup used in the computations. Nevertheless, it is possible to determine the underlying symmetry of the wave function by examination of the CI coefficients. In this case, the real component of the $^1\Delta_g$ state must have the $|\cdots1\pi_x^2 3\sigma_g^2\rangle$ and $|\cdots1\pi_y^2 3\sigma_g^2\rangle$ determinants appearing with equal coefficients but different signs, and the $^1\Sigma_g^+$ states have these coefficients appearing with the same sign (here we use labels σ and π for readability, but strictly speaking the computations are run under the D_{2h} point group). We have added a "state following" subroutine to our DETCI program[109] which allows the user to specify a series of determinants and coefficients, and the program will optimize the CASSCF for whichever root has the maximum overlap with the user-specified root. This allowed us to obtain CASSCF wave functions for the $^1\Delta_g$ state without difficulty.

To provide a good description of dynamical electron correlation on top of these qualitatively correct CASSCF reference functions, we obtained multireference configuration interaction (MRCI) wave functions using the CASSCF orbitals. We have used the second-order CI procedure, which generates all single and double substitutions out of all determinants which are present in the CASSCF wave function; this is a kind of "complete limit" for multireference configuration interaction with singles and doubles (MRCISD). The MRCI wave functions comprised 270 388 determinants. CASSCF and MRCI results were obtained using the DETCI and DETCAS modules of PSI 3.2.[110]

To explore somewhat less computationally demanding models, we also consider the MRPT approach through second-order based on CASSCF references. The most commonly used approach of this type is the CASPT2 method of Roos and co-workers.[67–70] Here we employ Celani and

Werner's[111] variation on this approach (which exploits a different internal contraction scheme to avoid the use of third and fourth order density matrices) as implemented in the MOLPRO program.[112] We found it technically easier to perform these computations using CASSCF orbitals averaged over all three states (the two $^1\Sigma_g^+$ states and the $^1\Delta_g$ state). Although, in principle, the $B\,^1\Delta_g$ state would be described more accurately without the admixture of $^1\Sigma_g^+$ orbitals in the SA-CASSCF procedure, we found in tests of the multireference CI energies that this led only to modest ($\sim10\%$) increases in the error for the $B\,^1\Delta_g$ state with essentially no change in the error for the $^1\Sigma_g^+$ states.

As mentioned in the Introduction, one of the goals of this study is to test the single-reference CR-CC and CR-EOMCC methods against the full CI and multireference data. The CR-CC and CR-EOMCC methods are based on the idea of improving the results of standard CC and EOMCC (CCSD, EOMCCSD, etc.) calculations through the suitably defined corrections to CC and EOMCC energies derived from the MMCC formalism,[18,19,25,28,56,57] which provides us with the explicit expressions for the differences between the CC or EOMCC and full CI energies of the electronic states of interest. As it turns out, these energy differences and the noniterative corrections to CC and EOMCC energies that result from them can be expressed in terms of the generalized moments of the CC or EOMCC equations characterizing a given CC/EOMCC approximation, i.e., the CC or EOMCC equations projected on the excited determinants that are not included in standard CC/EOMCC calculations. In the specific case of the CR-CCSD(T), CR-EOMCCSD(T), and CR-CCSD(TQ) methods considered in this work, we use the projections of the CCSD or EOMCCSD equations on the triply excited [the CR-CCSD(T) and CR-EOMCCSD(T) methods] or triply and quadruply excited [the CR-CCSD(TQ) approach] determinants to construct the relevant corrections to CCSD/EOMCCSD energies. Symbolically, the CR-CCSD(T) and CR-CCSD(TQ) energy formulas for the ground-state ($K=0$) problem can be written as

$$E_0 = E_0^{\text{CCSD}} + N_0/D_0, \tag{1}$$

and the corresponding CR-EOMCCSD(T) energies of excited ($K>0$) states have the general form

$$E_K = E_K^{\text{EOMCCSD}} + N_K/D_K. \tag{2}$$

Here, E_0^{CCSD} and E_K^{EOMCCSD} are the CCSD and EOMCCSD energies, respectively, and the numerator and denominator terms, N_K and D_K, respectively, that are used to calculate the corrections due to triple excitations [the CR-CCSD(T)/CR-EOMCCSD(T) case] or triple and quadruple excitations [the CR-CCSD(TQ) case] have been defined elsewhere.[18–20,24,25,27,28,58] The projections of the CCSD and EOMCCSD equations on triply or triply and quadruply excited determinants defining the corresponding moments of these equations enter the numerator terms N_K. In particular, the numerator N_0 entering the CR-CCSD(T) formula is similar to the triples correction to CCSD energy exploited in the standard CCSD(T) approximation. The numerator N_0 entering the CR-CCSD(TQ) energy expression is similar to the combined triples and quadruples correction defining the

CCSD(TQ_f) approach. Thus, the main difference between the standard CCSD(T) and CCSD(TQ_f) approaches on the one hand and the CR-CCSD(T) and CR-CCSD(TQ) methods on the other hand is the presence of the denominator D_0 in Eq. (1), which does not enter the CCSD(T) and CCSD(TQ_f) energy formulas. It is this denominator that renormalizes the triples and quadruples corrections, which allows the CR-CCSD(T) and CR-CCSD(TQ) methods to improve upon the failing of the standard CCSD(T) and CCSD(TQ_f) approaches in the bond-breaking region.[18–20]

In analogy to the standard CCSD(T) and CCSD(TQ_f) approaches, the CR-CCSD(T), CR-EOMCCSD(T), and CR-CCSD(TQ) methods are single-reference black-box schemes. In particular, the numerator and denominator terms, N_K and D_K, respectively, defining these methods are expressed in terms of the singly (T_1) and doubly (T_2) excited clusters obtained in the standard CCSD calculations and, in the case of excited-state ($K > 0$) calculations, the zero-, one-, and two-body components of the linear excitation operator R_K that defines the excited-state wave function in the EOM-CCSD ansatz. The straightforward relationship between the standard and completely renormalized CCSD(T) and CCSD(TQ) approaches implies that the computer costs of the CR-CCSD(T), CR-EOMCCSD(T), and CR-CCSD(TQ) calculations are essentially identical to the costs of the standard CCSD(T) and CCSD(TQ_f) calculations. Thus, in analogy to the CCSD(T) approach, the CR-CCSD(T) and CR-EOMCCSD(T) methods are $n_o^3 n_u^4$ procedures in the noniterative steps involving triples and $n_o^2 n_u^4$ procedures in the iterative CCSD and EOMCCSD steps (n_o and n_u are the numbers of occupied and unoccupied orbitals, respectively, used in the correlated calculations). More specifically, the CPU time required to calculate a triples correction to the CCSD or EOM-CCSD energy of a given (ground or excited) electronic state that defines one of the CR-CCSD(T) or CR-EOMCCSD(T) approaches[18,19,28,58] is twice the CPU time required to calculate the standard (T) correction of the ground-state CCSD(T) theory. Similarly, in complete analogy to the noniterative triples corrections, the costs of the CR-CCSD(TQ) calculations are of the same type as the costs of the CCSD(TQ_f) calculations [recall that CCSD(TQ_f) is an $n_o^3 n_u^4$ procedure in the triples part and an $n_o^2 n_u^5$ procedure in the noniterative steps involving quadruples[33]]. Again, all variants of the CR-CCSD(TQ) method[18–20,24,25,27,28] are twice as expensive as the CCSD(TQ_f) approach in the steps involving the noniterative triples and quadruples corrections.

In this paper, we focus on the performance of variant III of the CR-EOMCCSD(T) theory [the CR-EOMCCSD(T),III approach] and its ground-state CR-CCSD(T),III analog described in Refs. 28 and 58. Other variants of the CR-EOMCCSD(T) method described in Refs. 28 and 58, particularly the CR-EOMCCSD(T),ID approximation and its ground-state CR-CCSD(T),ID analog, provide similar results, which are not, therefore, reported here. The more substantial difference between the most complete variants of the CR-CCSD(T)/CR-EOMCCSD(T) theory, including the CR-CCSD(T),III/CR-EOMCCSD(T),III approximation examined in this work and the CR-CCSD(T),ID/CR-EOMCCSD(T),ID approach, and other CR-CCSD(T)/CR-

EOMCCSD(T) methods introduced in Refs. 28 and 58 is their behavior in the vicinity of the avoided crossing involving the $X\,^1\Sigma_g^+$ and $B'\,^1\Sigma_g^+$ states. We comment on this aspect of the CR-CCSD(T)/CR-EOMCCSD(T) calculations in Sec. III.

The CR-CCSD(T),III and CR-EOMCCSD(T),III approaches are somewhat more expensive than other CR-CCSD(T)/CR-EOMCCSD(T) calculations, since the CPU time required to calculate each triples correction is increased by the iterative $n_o^2 n_u^4$ steps of the single-reference CISD calculations that are used, along with the CCSD/EOMCCSD calculations, to determine the corrections due to triples.[28,58] Our experience with various CR-CCSD(T)/CR-EOMCCSD(T) methods shows than the CR-CCSD(T),III approach is somewhat more accurate than the original CR-CCSD(T) approximation,[18,19] which can only be applied to the ground-state problem [the CR-CCSD(T),III method has a natural extension to excited states through the CR-EOMCCSD(T),III approach of Refs. 28 and 58]. A direct comparison of the CR-CCSD(T),III and CR-CCSD(T) results for the ground-state of C_2 in Sec. III confirms this observation. In order to examine the effect of connected quadruples on the results for C_2, we compare the CR-CCSD(T) and CR-CCSD(T),III results for the $X\,^1\Sigma_g^+$ state with those obtained with the CR-CCSD(TQ) approximation. Again, several variants of the CR-CCSD(TQ) method have been formulated,[18–20,24,25,27,28] but our calculations for C_2 do not show significant differences among them. Thus, in our discussion in Sec. III, we focus on variant "a" of the CR-CCSD(TQ) theory [the CR-CCSD(TQ),a method].[20,24,25,27,28] We have to limit our discussion of the CR-CCSD(TQ) calculations to the $X\,^1\Sigma_g^+$ state of C_2, since the extension of the CR-CCSD(TQ) theory to excited states has not been implemented yet.

All CR-CCSD(T), CR-EOMCCSD(T), and CR-CCSD(TQ) calculations reported in this paper as well as the corresponding CCSD, EOMCCSD, CCSD(T), and CCSD(TQ_f) calculations, have been performed with the CC/EOMCC modules described in Refs. 22, 58, 113, and 114 interfaced with the GAMESS (Ref. 115) and ACES II (Ref. 116) packages. In all CC/EOMCC calculations, the spin- and symmetry-adapted ground-state RHF determinant was used as a reference.

III. RESULTS AND DISCUSSION

A. Full CI benchmarks

Full CI potential curves for the $X\,^1\Sigma_g^+$, $B\,^1\Delta_g$, and $B'\,^1\Sigma_g^+$ states of C_2 are presented in Fig. 1 using the data of Ref. 3. The potential well for the $X\,^1\Sigma_g^+$ state is much deeper than that of the other two states, which have similar energies. All three states become energetically close around $R = 1.5$ Å (R is the C–C separation) and the $B\,^1\Delta_g$ state actually drops below the $X\,^1\Sigma_g^+$ state around 1.7 Å. These two states remain very close in energy (within 3 kcal mol^{-1}) as they approach the dissociation limit. The $X\,^1\Sigma_g^+$ and $B'\,^1\Sigma_g^+$ states form an avoided crossing at $R \approx 1.7$ Å (at $R = 1.7$ Å, the two states are separated by 10 kcal mol^{-1} only) and for $R > 1.7$ Å, the $B'\,^1\Sigma_g^+$ state begins to rise in energy relative to the other two,
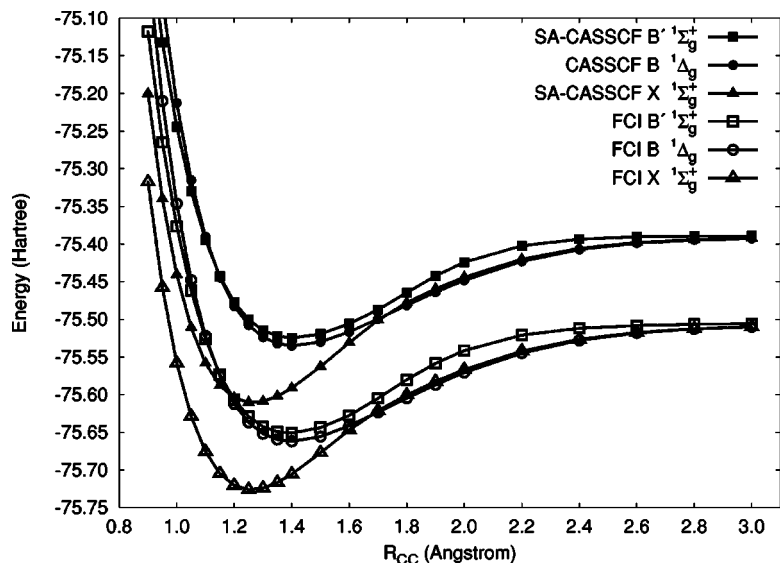
FIG. 1. CASSCF and FCI (full CI) potential curves for the $X\ ^1\Sigma_g^+$, $B\ ^1\Delta_g$, and $B'\ ^1\Sigma_g^+$ states of C_2.

but it approaches them again at larger distances. All three states approach the same asymptotic limit 2 $C(2s^2 2p^2\ ^3P)$ and are virtually degenerate (to within 2.5 kcal mol^{-1}) at $R=3.0$ Å.

The ground state features a surprisingly large multireference character even near equilibrium. At $R=1.25$ Å (the experimental equilibrium geometry is $R=1.243$ Å), the coefficient of the primary configuration $|(\text{core})2\sigma_g^2 2\sigma_u^2 1\pi_x^2 1\pi_y^2\rangle$ is only 0.83, and the doubly excited configuration $|(\text{core})2\sigma_g^2 1\pi_x^2 1\pi_y^2 3\sigma_g^2\rangle$ has a surprisingly large coefficient of 0.33. At this same geometry, the $B\ ^1\Delta_g$ state is dominated by $|(\text{core})2\sigma_g^2 2\sigma_u^2 1\pi_x^2 3\sigma_g^2\rangle - |(\text{core})2\sigma_g^2 2\sigma_u^2 1\pi_y^2 3\sigma_g^2\rangle$, while the $B'\ ^1\Sigma_g^+$ state has these two determinants dominant but with the same sign. Thus, in the equilibrium region both excited states are completely dominated by the $1\pi_u^2 \rightarrow 3\sigma_g^2$ double excitations relative to the primary configuration $|(\text{core})2\sigma_g^2 2\sigma_u^2 1\pi_x^2 1\pi_y^2\rangle$, whereas the ground state has a significantly quasidegenerate character involving the primary configuration and the $2\sigma_u^2 \rightarrow 3\sigma_g^2$ biexcited determinant.

The situation becomes even more complicated at larger C–C separations. By 1.6 Å, the doubly excited determinant $|(\text{core})2\sigma_g^2 1\pi_x^2 1\pi_y^2 3\sigma_g^2\rangle$ becomes much less important to the ground-state wave function, and the other two biexcited determinants $|(\text{core})2\sigma_g^2 2\sigma_u^2 1\pi_x^2 3\sigma_g^2\rangle$ and $|(\text{core})2\sigma_g^2 2\sigma_u^2 1\pi_y^2 3\sigma_g^2\rangle$, which also dominate the $B\ ^1\Delta_g$ and $B'\ ^1\Sigma_g^+$ states, are now much more important for the description of the $X\ ^1\Sigma_g^+$ state. Roughly speaking, the $B\ ^1\Delta_g$ and $B'\ ^1\Sigma_g^+$ states remain qualitatively similar to their form near the ground-state equilibrium geometry. However, by 1.80 Å, the $B\ ^1\Delta_g$ state has dropped below the $X\ ^1\Sigma_g^+$ state, and the character of the two $^1\Sigma_g^+$ states is reversed due to an avoided crossing. This gives the ground state potential curve a rather unusual shape which was not reproduced by any of the standard single-reference methods.[3]

In addition to the aforementioned configurations, several of the most important configurations in the full CI wave functions involve double excitations to the antibonding $1\pi_g$ orbitals. Thus it seems clear that the active space in multireference wave functions should include the $2\sigma_u$, $1\pi_u$, $3\sigma_g$, $1\pi_g$, and $3\sigma_u$ orbitals. This accounts for the entire valence space except for the $2\sigma_g$ orbital, which generally remains doubly occupied in the most important electron configurations. We explored some additional multireference computations in which the $2\sigma_u$ orbital was left out of the active space.

B. Accuracy of CASSCF

Figure 1 presents CASSCF potential curves along with the exact, full CI curves. The corresponding energy values are given in Tables I–III (see Table I of Ref. 3 for the full CI data). State-averaged orbitals have been used for the two $^1\Sigma_g^+$ states. CASSCF is designed to provide a good description of electronic near degeneracies (nondynamical correlation), but it does not provide a reliable treatment of short-range dynamical correlation. Hence, the CASSCF energies are significantly higher than the full CI energies. Nevertheless, Fig. 1 demonstrates that the qualitative features of all three states are accurately represented by the CASSCF wave functions. A more quantitative assessment is provided by Fig. 2, which displays the error in the CASSCF curves vs full CI; because a constant shift in the curve would not affect any chemical properties, the most important issue is the flatness of the error curves. None of the error curves are close to being flat: the error for the $X\ ^1\Sigma_g^+$ state shows significant changes at intermediate distances, and the errors for the $B\ ^1\Delta_g$ and $B'\ ^1\Sigma_g^+$ states are significantly larger at short distances than at larger distances. Nevertheless, the CASSCF wave functions clearly provide reasonable reference functions which might be further improved by multireference models of dynamical correlation. Indeed, the larger errors at short distances observed for the $B\ ^1\Delta_g$ and $B'\ ^1\Sigma_g^+$ states are consistent with the expectation that dynamical correlation should be larger at these geometries (because electrons are closer together). If we quantify the flatness of the error curves by the NPE, we obtain values of 5.4, 11.3, and 11.0 kcal mol^{-1} for the $X\ ^1\Sigma_g^+$, $B\ ^1\Delta_g$, and $B'\ ^1\Sigma_g^+$ states, respectively (see Table IV). These NPEs are quite sizable, although they are all much smaller than the NPE of 21.6 kcal mol^{-1} computed for the $X\ ^1\Sigma_g^+$ state using the UHF CCSD(T) method, not to mention the NPE of 61.3 kcal mol^{-1} obtained for this state with the RHF

TABLE I. Total energies (hartrees) for the $X\,{}^1\Sigma_g^+$ state of C_2 for various values of the internuclear separation $R(C-C)$ (Å) using the 6-31G* basis set.

$R(C-C)$	SA-CASSCF	SA-CASPT2	MRCI	CCSD	CR(T),III[a]	CR(T)[b]	CR(TQ),a[c]
0.90	−75.200 369	−75.311 743	−75.314 659	−75.290 119	−75.310 307	−75.308 053	−75.310 362
0.95	−75.340 031	−75.451 828	−75.454 710	−75.430 310	−75.450 482	−75.448 178	−75.450 750
1.00	−75.440 478	−75.552 552	−75.555 407	−75.530 942	−75.551 201	−75.548 810	−75.551 666
1.05	−75.510 846	−75.622 890	−75.625 762	−75.601 021	−75.621 472	−75.618 974	−75.622 129
1.10	−75.558 190	−75.669 846	−75.672 810	−75.647 606	−75.668 349	−75.665 726	−75.669 186
1.15	−75.587 907	−75.698 918	−75.702 046	−75.676 225	−75.697 336	−75.694 576	−75.698 343
1.20	−75.604 189	−75.714 430	−75.717 769	−75.691 204	−75.712 736	−75.709 833	−75.713 904
1.25	−75.610 330	−75.719 774	−75.723 349	−75.695 935	−75.717 918	−75.714 871	−75.719 243
1.30	−75.608 922	−75.717 612	−75.721 437	−75.693 083	−75.715 526	−75.712 341	−75.717 011
1.35	−75.602 006	−75.710 037	−75.714 120	−75.684 744	−75.707 631	−75.704 328	−75.709 290
1.40	−75.591 196	−75.698 699	−75.703 053	−75.672 564	−75.695 864	−75.692 469	−75.697 723
1.50	−75.562 720	−75.669 696	−75.674 696	−75.641 556	−75.665 564	−75.662 083	−75.667 923
1.60	−75.530 897	−75.638 349	−75.644 491	−75.607 318	−75.631 897	−75.628 434	−75.634 860
1.70	−75.501 051	−75.610 619	−75.618 641	−75.574 160	−75.600 722	−75.595 835	−75.602 805
1.80	−75.477 669	−75.588 855	−75.597 900	−75.544 554	−75.582 601	−75.566 777	−75.574 140
1.90	−75.459 434	−75.570 557	−75.579 896	−75.519 837	−75.564 922	−75.542 662	−75.550 095
2.00	−75.443 952	−75.554 833	−75.564 150	−75.500 618	−75.548 233	−75.524 199	−75.531 169
2.20	−75.420 247	−75.530 793	−75.539 687	−75.478 125	−75.516 428	−75.503 863	−75.507 815
2.40	−75.405 657	−75.515 579	−75.524 032	−75.470 669	−75.499 728	−75.498 762	−75.497 839
2.60	−75.397 903	−75.506 703	−75.515 044	−75.469 410	−75.500 407	−75.499 276	−75.493 526
2.80	−75.394 093	−75.501 701	−75.510 178	−75.469 749	−75.502 627	−75.500 809	−75.490 992
3.00	−75.392 204	−75.498 879	−75.507 543	−75.470 279	−75.504 778	−75.502 163	−75.488 999

[a]The CR-CCSD(T),III approach of Ref. 58.
[b]The CR-CCSD(T) approach of Refs. 18 and 19.
[c]The CR-CCSD(TQ),a approach of Ref. 20.

CCSD(T) approach[3] (cf. Table IV). The standard single-reference CC methods provide an accurate description of dynamical correlation, but they are incapable of describing nondynamical correlation effects, which play a significant role in reducing NPEs.

C. Accuracy of MRCI

As mentioned above, MRCI is a generally applicable method which, in principle, can provide very accurate results for almost any bond-breaking problem, as long as the computations do not become prohibitively expensive. In the case

TABLE II. Total energies (hartrees) for the $B\,{}^1\Delta_g$ state of C_2 for various values of the internuclear separation $R(C-C)$ (Å) using the 6-31G* basis set.

$R(C-C)$	CASSCF	SA-CASPT2	MRCI	EOMCCSD	CR-EOMCCSD(T),III
0.90	−74.893 331	−75.022 209	−75.025 398	−74.923 620	−75.013 169
0.95	−75.075 584	−75.202 397	−75.206 821	−75.106 101	−75.194 742
1.00	−75.212 794	−75.337 568	−75.343 207	−75.243 363	−75.331 441
1.05	−75.315 088	−75.437 989	−75.444 674	−75.345 438	−75.433 212
1.10	−75.390 288	−75.511 570	−75.519 046	−75.420 103	−75.507 921
1.15	−75.444 470	−75.564 363	−75.572 408	−75.473 413	−75.561 636
1.20	−75.482 382	−75.601 057	−75.609 519	−75.510 112	−75.599 097
1.25	−75.507 752	−75.625 341	−75.634 116	−75.533 931	−75.624 030
1.30	−75.523 521	−75.640 129	−75.649 152	−75.547 820	−75.639 363
1.35	−75.532 003	−75.647 725	−75.656 947	−75.554 113	−75.647 389
1.40	−75.535 020	−75.649 941	−75.659 328	−75.554 656	−75.649 893
1.50	−75.530 048	−75.643 602	−75.653 244	−75.544 028	−75.643 613
1.60	−75.516 606	−75.629 080	−75.638 904	−75.524 327	−75.628 935
1.70	−75.499 446	−75.611 105	−75.621 042	−75.500 808	−75.610 585
1.80	−75.481 343	−75.592 424	−75.602 394	−75.476 781	−75.591 009
1.90	−75.463 908	−75.574 614	−75.584 523	−75.454 314	−75.571 424
2.00	−75.448 079	−75.558 566	−75.568 312	−75.434 604	−75.552 505
2.20	−75.423 034	−75.533 262	−75.542 444	−75.404 752	−75.518 355
2.40	−75.407 258	−75.516 886	−75.525 515	−75.385 013	−75.490 553
2.60	−75.398 784	−75.507 299	−75.515 719	−75.371 184	−75.469 421
2.80	−75.394 618	−75.501 949	−75.510 444	−75.361 111	−75.455 525
3.00	−75.392 570	−75.498 970	−75.507 627	−75.353 777	−75.440 830

TABLE III. Total energies (hartrees) for the B' $^1\Sigma_g^+$ state of C_2 for various values of the internuclear separation R(C–C) (Å) using the 6-31G* basis set.

R(C–C)	SA-CASSCF	SA-CASPT2	MRCI	EOMCCSD	CR-EOMCCSD(T),III
0.90	−74.984 720	−75.112 772	−75.114 235	−75.060 845	−75.120 558
0.95	−75.132 145	−75.259 385	−75.261 307	−75.201 112	−75.265 143
1.00	−75.244 195	−75.370 171	−75.373 023	−75.303 995	−75.373 763
1.05	−75.329 841	−75.454 183	−75.458 303	−75.379 983	−75.455 960
1.10	−75.394 786	−75.517 397	−75.522 719	−75.436 717	−75.517 932
1.15	−75.442 826	−75.563 818	−75.570 064	−75.478 630	−75.563 614
1.20	−75.477 044	−75.596 588	−75.603 497	−75.508 204	−75.596 030
1.25	−75.500 169	−75.618 426	−75.625 809	−75.527 448	−75.617 766
1.30	−75.514 571	−75.631 675	−75.639 402	−75.538 295	−75.631 058
1.35	−75.522 236	−75.638 296	−75.646 272	−75.542 532	−75.637 784
1.40	−75.524 785	−75.639 888	−75.648 033	−75.541 711	−75.639 488
1.50	−75.519 434	−75.632 784	−75.641 011	−75.529 872	−75.632 589
1.60	−75.505 721	−75.617 228	−75.624 913	−75.510 561	−75.618 162
1.70	−75.487 174	−75.595 899	−75.602 356	−75.488 773	−75.599 216
1.80	−75.464 557	−75.571 686	−75.577 681	−75.467 574	−75.570 014
1.90	−75.442 230	−75.550 015	−75.556 017	−75.448 733	−75.545 667
2.00	−75.424 148	−75.532 769	−75.539 043	−75.433 102	−75.526 848
2.20	−75.402 242	−75.511 229	−75.518 365	−75.411 294	−75.505 502
2.40	−75.393 423	−75.501 453	−75.509 427	−75.397 887	−75.496 517
2.60	−75.390 336	−75.497 324	−75.505 820	−75.388 720	−75.479 074
2.80	−75.389 325	−75.495 541	−75.504 309	−75.382 197	−75.467 128
3.00	−75.389 046	−75.494 728	−75.503 640	−75.377 616	−75.459 577

of the C_2 molecule, the small size of the system makes even a second-order CI easily accessible. MRCI wave functions have been computed using the CASSCF orbitals for the B $^1\Delta_g$ state and SA-CASSCF orbitals for the two $^1\Sigma_g^+$ states. The MRCI potential curves are of very high quality, and we do not present a figure of the total energies because they are impossible to distinguish from the full CI energies. Instead, we plot the errors vs full CI in Fig. 3. The actual MRCI energies are provided in Tables I–III.

The MRCI errors are much smaller than the CASSCF errors, and the error curves are also much flatter, with differences of less than 1 kcal mol^{-1} between the maximum and minimum errors. Errors are somewhat larger at smaller distances, and the general behavior of the error is similar for each of the three states. The NPEs in Table IV are 0.4, 0.6,

and 0.7 kcal mol^{-1} for the X $^1\Sigma_g^+$, B $^1\Delta_g$, and B' $^1\Sigma_g^+$ states, respectively. These NPEs are somewhat higher than our best MRCI results for bond-breaking reactions in BH, CH$_4$, and HF (NPEs of 0.3 kcal mol^{-1} or less),[65] but that is to be expected because the electronic structure of C_2 is much more complex. The reliability of MRCI is very satisfactory even for this difficult test case. The high accuracy of the MRCI results and the significant reduction of NPEs compared to the underlying CASSCF calculations clearly illustrate the importance of a well-balanced description of the nondynamical and dynamical correlation effects in studies of molecular potential energy surfaces. CASSCF describes only the nondynamical correlation effects and this results in a significant increase of errors and, what is perhaps most important, relatively large NPE values compared to MRCI.
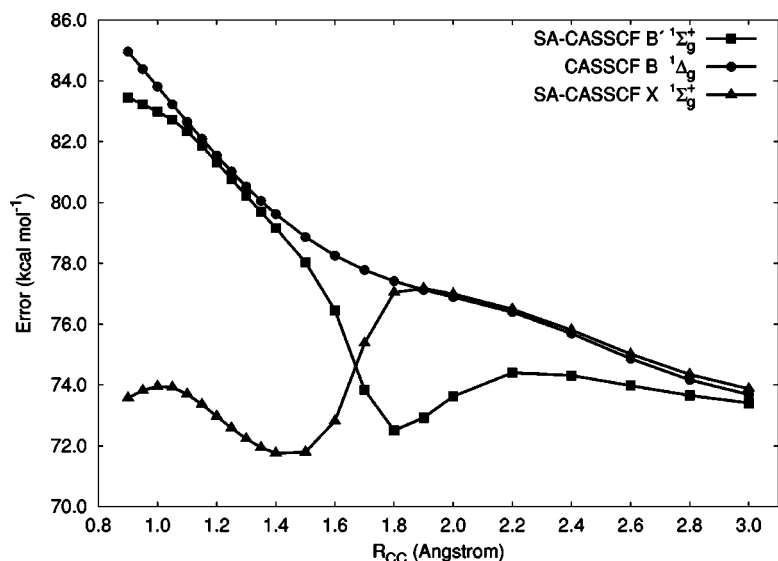

FIG. 2. Errors in CASSCF potential curves for the X $^1\Sigma_g^+$, B $^1\Delta_g$, and B' $^1\Sigma_g^+$ states of C_2.

TABLE IV. Nonparallelity errors (kcal mol^{-1}) vs full CI for three states of C_2 using the 6-31G* basis set.

Method	$X\,{}^1\Sigma_g^+$	$B\,{}^1\Delta_g$	$B'\,{}^1\Sigma_g^+$
(SA)-CASSCF	5.4	11.3	11.0
(SA)-CASSCF MRCI	0.4	0.6	0.7
SA-CASPT2	3.8	3.6	4.0
(EOM)CCSD	24.3	34.1	44.9
(EOM)CCSD[a]	24.2	20.7	22.5
(EOM)CCSD[b]	17.5	16.3	17.4
CR-(EOM)CCSD(T),III	13.5	35.9	30.9
CR-(EOM)CCSD(T),III[a]	8.4	3.8	7.5
CR-(EOM)CCSD(T),III[b]	8.3	1.3	2.1
CR-(EOM)CCSD(T),IIA	21.2	37.3	33.4
CR-(EOM)CCSD(T),IIA[a]	19.9	16.6	10.3
CR-(EOM)CCSD(T),IIA[b]	14.0	10.9	6.7
CCSD(T)	61.3		
CCSD(T)[a]	14.5		
CCSD(T)[b]	11.4		

[a]Based on the results in the $R=1.0-2.0$ Å region.
[b]Based on the results in the $R=1.1-1.8$ Å region.

The high quality of these MRCI results is not often possible to achieve for larger molecules because the second-order CI procedure is very expensive computationally. Various schemes exist for reducing the costs of MRCI computations, from internal contraction[117] to neglecting references with small weights. We briefly examined the CISD[TQ] wave function,[118–120] which is a "class-selected" MRCI wave function in which higher-than-quadruply substituted determinants are neglected along with determinants which place more than two electrons outside the active space. In CISD[TQ] computations of the two ${}^1\Sigma_g^+$ states (87 415 determinants), the NPEs grow dramatically to 16 kcal mol^{-1} (X state) and 24 kcal mol^{-1} (B' state), suggesting that this selection scheme is not robust enough to handle the breaking of the double bond in the C_2 molecule. The performance of the CISD[TQ] wave function is much better for breaking single bonds in BH, HF, and CH$_4$.[65]

D. Accuracy of CASPT2

A somewhat more computationally affordable alternative to MRCI is the CASPT2 approach. Using the MOLPRO (Ref. 112) implementation of CASPT2 with state-averaged orbitals for all three states, we obtain potential curves which are approximately parallel to the full CI curves and are shifted slightly higher in energy. We omit a figure of these curves because the near degeneracies beyond 1.6 Å make them hard to distinguish. However, the error curves are plotted in Fig. 4 (see Tables I–III for the corresponding total energies). Unlike the MRCI errors of Fig. 3, which were largest at small distances, here the errors are greatest at intermediate or larger distances. The NPEs in Table IV are 3.8, 3.6, and 4.0 kcal mol^{-1} for the $X\,{}^1\Sigma_g^+$, $B\,{}^1\Delta_g$, and $B'\,{}^1\Sigma_g^+$ states, respectively. If we attempt to reduce the size of the active space by making the $2\sigma_g$ orbital inactive, NPEs for the three states grow to 8.1, 7.3, and 6.3 kcal mol^{-1}, respectively, indicating significant sensitivity to the choice of active space for this difficult system. A more general exploration of the sensitivity of CASPT2 and MRCI results to the choice of active space has been presented previously.[65,66] The NPEs for CASPT2 are significantly improved over the NPEs for CASSCF, but they are not nearly as good as the MRCI results. Nevertheless, this type of accuracy is probably suffi-
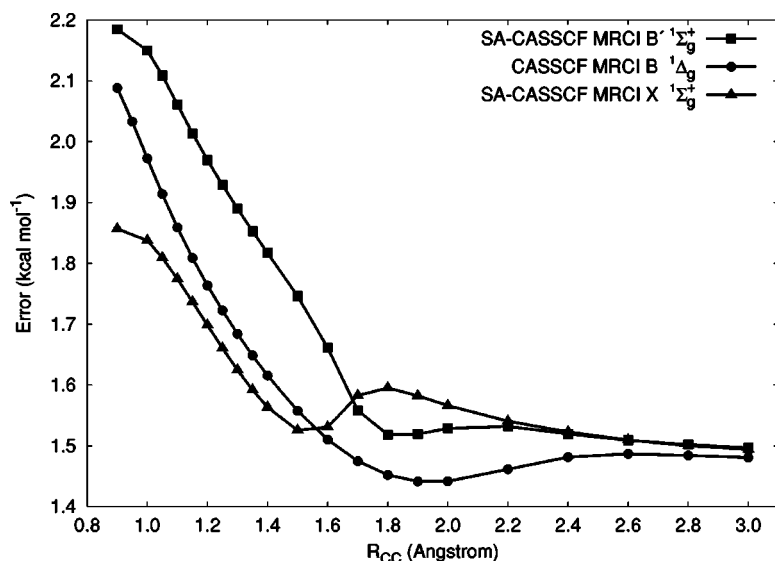
FIG. 3. Errors in multireference CI potential curves for the $X\,{}^1\Sigma_g^+$, $B\,{}^1\Delta_g$, and $B'\,{}^1\Sigma_g^+$ states of C_2.
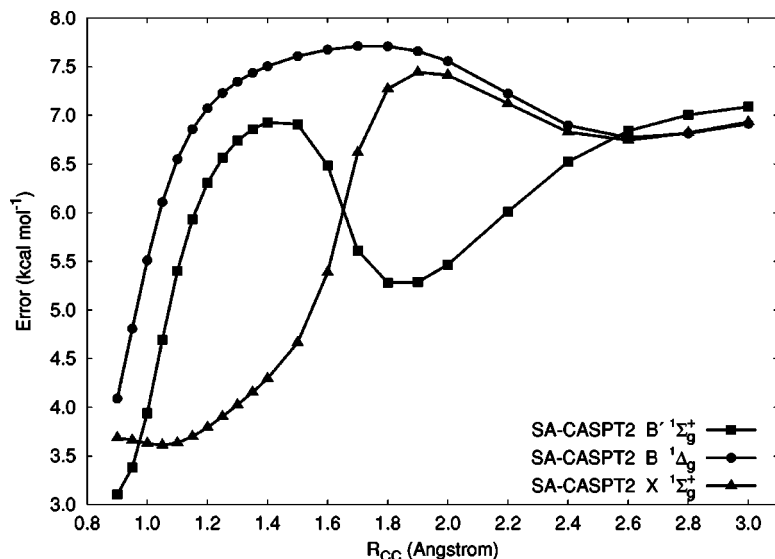
FIG. 4. Errors in CASPT2 potential curves for the $X\ ^1\Sigma_g^+$, $B\ ^1\Delta_g$, and $B'\ ^1\Sigma_g^+$ states of C_2 (using state-averaged orbitals for all three states).

cient for many applications. The CASPT2 NPEs for C_2 are similar to those found for the much simpler cases of bond breaking in BH, CH_4, and HF ($0.5-3.3$ kcal mol^{-1}), indicating that the CASPT2 method is robust and does not degrade significantly for molecules with greater degrees of nondynamical correlation.

We note that the CASPT2 method is a "diagonalize then perturb," single-state approach, which can have some difficulties when states become nearly degenerate.[121] In the present case, the SA-CASSCF (and CASPT2) energies become close at large distances because all three states correlate to the same asymptotic limit. Nevertheless, the present CASPT2 energies appear to be reliable for the states and geometries considered. The significant reduction of absolute errors (from ca. $72-85$ to $3-8$ kcal mol^{-1}) and NPEs (from ca. $5-11$ to 4 kcal mol^{-1}) compared to the underlying CASSCF calculations shows that CASPT2 provides a reasonably balanced description of the nondynamical and dynamical correlation effects, needed in calculations of molecular potential energy surfaces. As a result, all important features of the three states of C_2 examined in this paper are correctly reproduced by the CASPT2 approach. In particular, as in the full CI case, the $B\ ^1\Delta_g$ state drops below the $X\ ^1\Sigma_g^+$ state around $R=1.7$ Å. The energy separation between the $X\ ^1\Sigma_g^+$ and $B'\ ^1\Sigma_g^+$ states in the vicinity of the avoided crossing at $R\approx 1.7$ Å obtained with CASPT2, of 9 kcal mol^{-1}, is very similar to that obtained with the full CI method (10 kcal mol^{-1}).

E. Accuracy of completely renormalized coupled-cluster methods

Multireference methods, such as MRCI and CASPT2, which are specifically designed to handle quasidegenerate ground and excited states, work well for the $X\ ^1\Sigma_g^+$, $B\ ^1\Delta_g$, and $B'\ ^1\Sigma_g^+$ states of C_2, eliminating the failures of single-reference approaches discussed in the earlier paper,[3] but we must keep in mind that they are not as easy to use as the single-reference methods and they can be prohibitively expensive, particularly when one has to use larger active orbital spaces. The question arises if one can improve the results of

single-reference calculations for the complicated $X\ ^1\Sigma_g^+$, $B\ ^1\Delta_g$, and $B'\ ^1\Sigma_g^+$ states of C_2 without resorting to multireference techniques. This question is addressed in this section, where we compare the results of the single-reference, black-box, CR-CCSD(T), CR-EOMCCSD(T), and CR-CCSD(TQ) calculations employing the spin- and symmetry-adapted RHF reference with full CI and multireference results.

Clearly, the CR-CCSD(T), CR-EOMCCSD(T), and CR-CCSD(TQ) methods, which are all based on the idea of adding simple noniterative corrections due to triples or triples and quadruples to CCSD or EOMCCSD energies, face a significant challenge. This challenge is illustrated in Fig. 5(a), where we compare the CCSD and EOMCCSD potential curves for the $X\ ^1\Sigma_g^+$, $B\ ^1\Delta_g$, and $B'\ ^1\Sigma_g^+$ states of C_2 with the corresponding full CI potentials (the actual CCSD and EOMCCSD energies are given in Tables I–III). As one can see, the CCSD and EOMCCSD potentials are not only characterized by huge errors and large NPE values (cf. the discussion below); they are also qualitatively incorrect. For example, the $B\ ^1\Delta_g$ potential curve is shifted to higher energies so much that it crosses the $B'\ ^1\Sigma_g^+$ curve; this is completely wrong since we know from the full CI calculations that the $B\ ^1\Delta_g$ curve should cross the $X\ ^1\Sigma_g^+$ potential, not the $B'\ ^1\Sigma_g^+$ curve. The small, ~10 kcal mol^{-1} energy gap corresponding to an avoided crossing of the $X\ ^1\Sigma_g^+$ and $B'\ ^1\Sigma_g^+$ full CI states at $R\approx 1.7$ Å is absent in the CCSD/EOMCCSD results. According to the CCSD/EOMCCSD calculations, the closest approach of the $X\ ^1\Sigma_g^+$ and $B'\ ^1\Sigma_g^+$ potentials should occur in the $R=2.0-2.2$ Å region, where both states are separated by more than 40 kcal mol^{-1}. Again, this is completely incorrect, showing that a large amount of nondynamical and dynamical correlation is missing in the CCSD/EOMCCSD calculations. The extremely poor performance of the standard EOMCCSD approach for the $B\ ^1\Delta_g$ and $B'\ ^1\Sigma_g^+$ states of C_2 confirms the fact that EOMCCSD cannot describe excited-state potential energy surfaces along bond-breaking coordinates and excited states dominated by two-electron transitions (in this case, the $1\pi_u^2 \rightarrow 3\sigma_g^2$ double excitations relative to the RHF determinant).

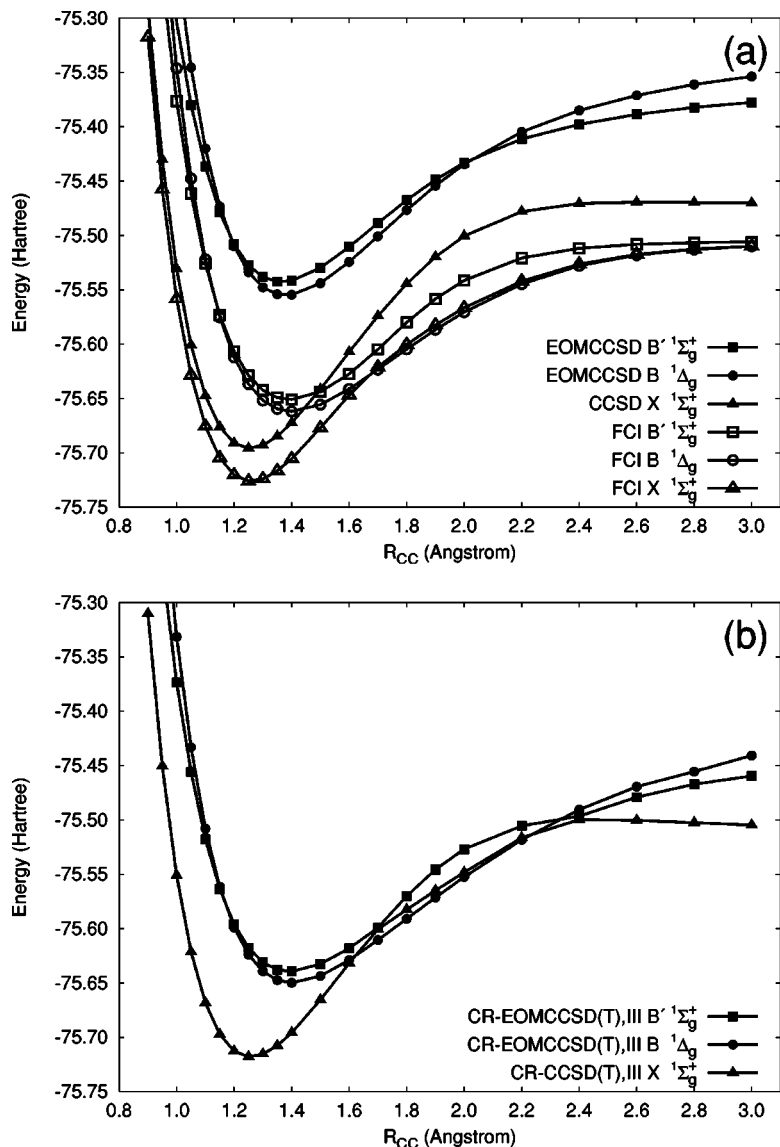The CR-EOMCCSD(T),III approach and its ground-state

FIG. 5. CCSD/EOMCCSD and FCI (full CI) (a) and CR-CCSD(T),III/CR-EOMCCSD(T),III (b) potential curves for the $X\,^1\Sigma_g^+$, $B\,^1\Delta_g$, and $B'\,^1\Sigma_g^+$ states of C_2.

CR-CCSD(T),III variant improve the poor CCSD/EOMCCSD results quite dramatically. This can be seen by comparing the CCSD/EOMCCSD and full CI potential energy curves in Fig. 5(a) with the CR-CCSD(T),III/CR-EOMCCSD(T),III potentials shown in Fig. 5(b) and by analyzing the errors in the CCSD/EOMCCSD and CR-CCSD(T),III/CR-EOMCCSD(T),III results shown in Fig. 6 [the actual CR-CCSD(T),III/CR-EOMCCSD(T),III energies are given in Tables I–III]. Although the CR-EOMCCSD(T),III method cannot accurately describe the $B\,^1\Delta_g$ and $B'\,^1\Sigma_g^+$ excited states in the asymptotic region [the CR-CCSD(T),III results for the $X\,^1\Sigma_g^+$ state seem to be considerably better in this region], the CR-CCSD(T),III/CR-EOMCCSD(T),III results in the $R \leqslant 2.0$ Å region are excellent, particularly considering the single-reference black-box nature and the relatively low cost of the CR-CCSD(T),III/CR-EOMCCSD(T),III calculations and the challenge that the electronic states of C_2 create for such approaches. The CR-CCSD(T),III/CR-EOMCCSD(T),III approach is capable of restoring the crossing of the $X\,^1\Sigma_g^+$ and $B\,^1\Delta_g$ states, which occurs at 1.62 Å, in reasonable agreement with full CI. It also brings the $X\,^1\Sigma_g^+$ and $B'\,^1\Sigma_g^+$ states much closer to each

other in the $R=1.6-1.8$ Å region, trying to mimic the existence of the avoided crossing between these two states that the standard CCSD/EOMCCSD methods fail to describe (cf. the end of this section for further remarks).

The reasonable performance of the CR-CCSD(T),III and CR-EOMCCSD(T),III methods can be seen if we analyze the errors relative to full CI (cf. Fig. 6) and the corresponding NPE values (see Table IV). If we ignore the asymptotic region, the unsigned errors in the $R \leqslant 2.0$ Å region characterizing the CR-CCSD(T),III and CR-EOMCCSD(T),III results for the ground and excited states of C_2 examined in this work are quite small. The errors in the CR-CCSD(T),III results for the $X\,^1\Sigma_g^+$ state vary between 4.5 and 12.8 kcal mol^{-1}. The standard RHF CCSD(T) approach can lower these errors to as little as 1.2 kcal mol^{-1} in the equilibrium region, but the unsigned errors in the CCSD(T) results rapidly increase with the C–C separation, to 14.7 kcal mol^{-1} at $R=2.0$ Å and 46.6 kcal mol^{-1} at $R=3.0$ Å. In consequence, the NPE value characterizing the CR-CCSD(T),III approximation (13.5 kcal mol^{-1}) is much lower than that obtained in the RHF CCSD(T) calculations (61.3 kcal mol^{-1}). In fact, the NPE value obtained with the RHF-based CR-CCSD(T),III
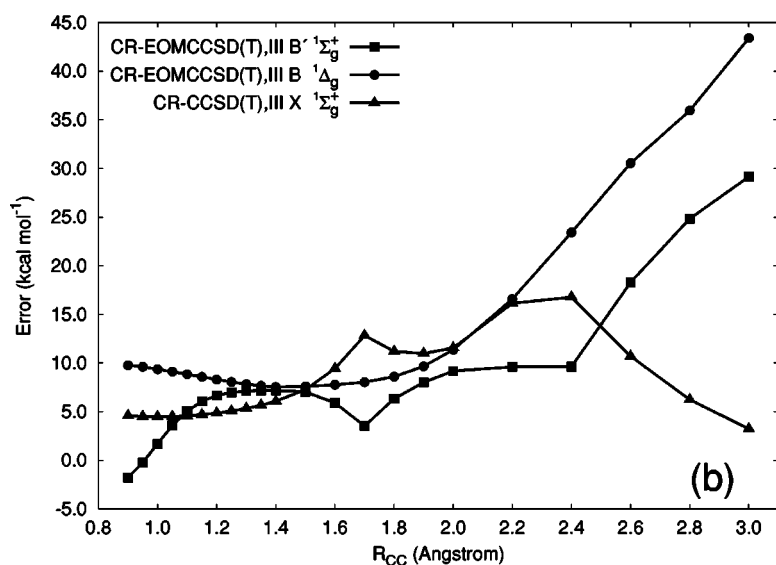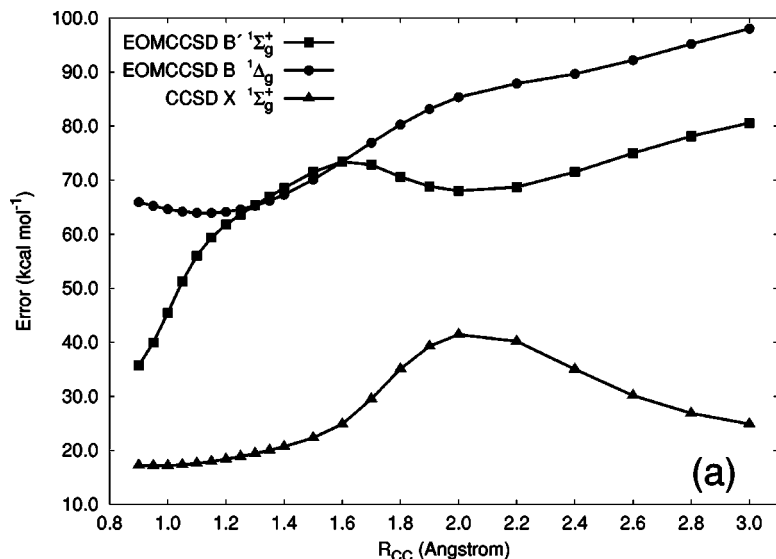
FIG. 6. Errors in CCSD/EOMCCSD (a) and CR-CCSD(T),III/CR-EOMCCSD(T),III (b) potential curves for the $X\,^1\Sigma_g^+$, $B\,^1\Delta_g$, and $B'\,^1\Sigma_g^+$ states of C_2.

approach is also considerably smaller than that obtained with the UHF CCSD(T) method (21.6 kcal mol^{-1}; see Ref. 3). This shows once again that we may be better off by using spin- and symmetry-adapted references of the RHF type in single-reference calculations when potential energy curves are examined. If we limit ourselves to the $R=1.0$–2.0 Å region, the NPE value obtained in the RHF CCSD(T) calculations reduces to 14.5 kcal mol^{-1}, which is much better than the 61.3 kcal mol^{-1} obtained in the entire $R=0.9$–3.0 Å region, but the CR-CCSD(T),III approach continues to remain a better method even in this case, producing the NPE of 8.4 kcal mol^{-1} (see Table IV).

We tried to examine if we could improve the NPE values resulting from the CR-CCSD(T),III calculations for the $X\,^1\Sigma_g^+$ state further by incorporating the connected quadruply excited clusters via the standard and completely renormalized CCSD(TQ) methods (see Fig. 7 and Table I), but neither the standard CCSD(TQ$_f$) approximation nor the CR-CCSD(TQ),a method produced the small NPE values of the CASPT2 or MRCI quality over a wide region of geometries considered in this work. The NPE values characterizing CCSD(TQ$_f$) and CR-CCSD(TQ),a methods are 21.5 and

18.2 kcal mol^{-1}, respectively. The CR-CCSD(TQ),a value of NPE is actually somewhat worse than that obtained with the CR-CCSD(T),III approach. This is a consequence of the fact that the CR-CCSD(TQ),a approximation has been developed^{20} by augmenting the original version of the CR-CCSD(T) method of Refs. 18 and 19, which is less accurate than the CR-CCSD(T),III approach in the region of the intermediate R values [cf. the CR-CCSD(T),III and CR-CCSD(T) potential energy and error curves in Fig. 7]. This is telling us that it may be useful to incorporate quadruples in the CR-CCSD(T),III scheme. On the other hand, the CR-CCSD(TQ),a approach significantly improves the potential energy curve for the $X\,^1\Sigma_g^+$ state obtained in the standard CCSD(TQ$_f$) calculations, which is located above the full CI curve at shorter C–C distances while going ≈ 7 kcal mol^{-1} below the full CI curve at larger values of R. The original CR-CCSD(T) and CR-CCSD(TQ),a approaches provide a smoother description of the $X\,^1\Sigma_g^+$ state in the avoided crossing region compared to the newer CR-CCSD(T),III approximation of Ref. 58, but this is accomplished at the expense of increasing the errors relative to full CI. Thus, we must con-
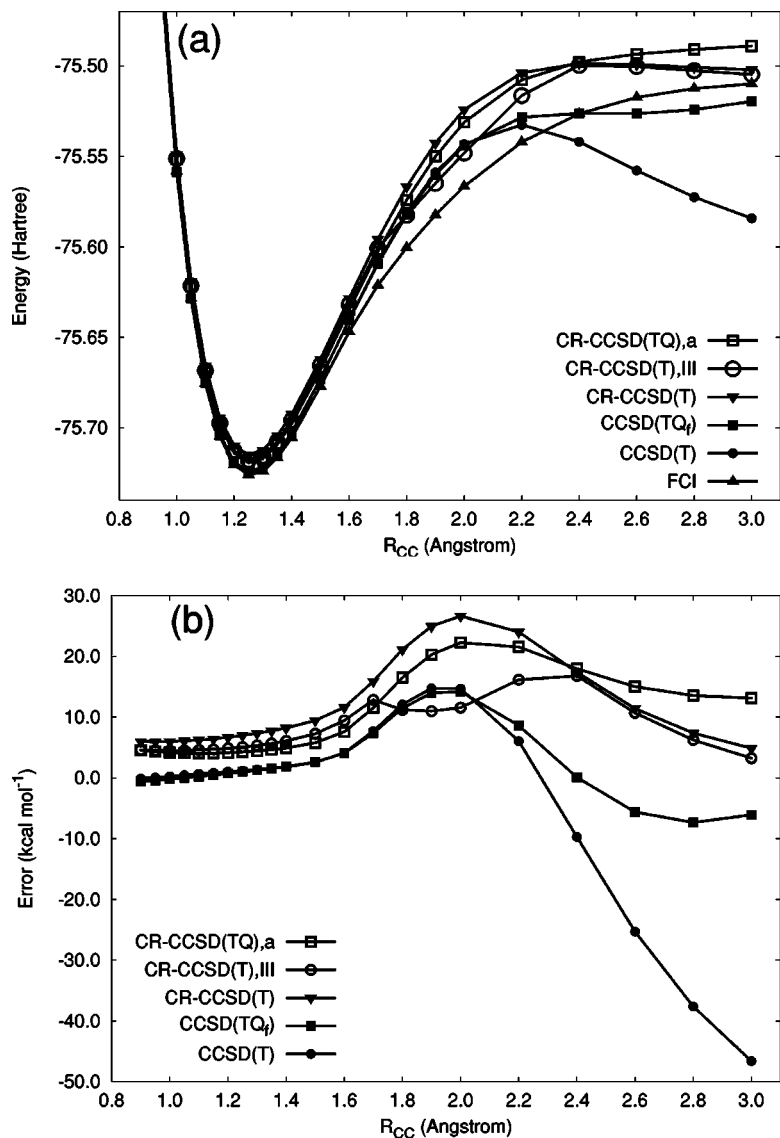
FIG. 7. A comparison of the ground-state potential curves obtained with the standard CCSD(T) and CCS-D(TQ) methods and their completely renormalized CR-CCSD(T), CR-CCSD(T),III, and CR-CCSD(TQ),*a* analogs with the exact, FCI (full CI) curve: (a) potential energy curves, (b) errors relative to FCI.

clude at this time that while the CR-CCSD(TQ),*a* approach that describes the combined effect of triples and quadruples provides a smoother and asymptotically correct potential curve for the $X\ ^1\Sigma_g^+$ state, the newer CR-CCSD(T),III approximation, in which quadruples are ignored, is characterized by smaller errors and smaller NPE values, which are on the same order of magnitude as those resulting from multireference CASSCF/CASPT2 calculations.

Let us now discuss the errors and NPE values obtained in the CR-EOMCCSD(T),III calculations for the $B\ ^1\Delta_g$ and $B'\ ^1\Sigma_g^+$ states [see Fig. 6(b)]. As already mentioned, the CR-EOMCCSD(T),III approach has difficulties in describing the asymptotic region in this case, which is a consequence of the extremely poor description of the $B\ ^1\Delta_g$ and $B'\ ^1\Sigma_g^+$ states by the underlying EOMCCSD method, but the CR-EOMCCSD(T),III results in the somewhat narrower $R \leqslant 2.0$ Å region are excellent. For the $B\ ^1\Delta_g$ state, the errors in the CR-EOMCCSD(T),III results in the $R \leqslant 2.0$ Å region vary between 7.5 and 11.4 kcal mol^{-1}. Similar errors for the $B'\ ^1\Sigma_g^+$ state vary between -1.8 and 9.2 kcal mol^{-1}. This should be compared to the 63.9–85.3 kcal mol^{-1} and 35.7–73.4 kcal mol^{-1} errors obtained for the $B\ ^1\Delta_g$ and

$B'\ ^1\Sigma_g^+$ states, respectively, in the $R \leqslant 2.0$ Å region with the EOMCCSD approach. If we limit ourselves to the $R = 1.0$–2.0 Å region, the NPE value resulting from the CR-EOMCCSD(T),III calculations for the $B\ ^1\Delta_g$ state reduces to 3.8 kcal mol^{-1}, which is a result of CASPT2 quality. For the $B'\ ^1\Sigma_g^+$ state, we obtain 7.5 kcal mol^{-1} in the same region. If we focus on the spectroscopically important $R = 1.1$–1.8 Å region, which is wide enough to include the minima on the $X\ ^1\Sigma_g^+$, $B\ ^1\Delta_g$, and $B'\ ^1\Sigma_g^+$ curves and the region of curve crossing/avoided crossing, the NPE values resulting from CR-EOMCCSD(T),III calculations are 1.3 kcal mol^{-1} for the $B\ ^1\Delta_g$ state and 2.1 kcal mol^{-1} for the $B'\ ^1\Sigma_g^+$ state. Thus, the CR-EOMCCSD(T),III approach is capable of providing results of near-MRCI quality for these two states if the asymptotic region is ignored. This is an important finding for applications of the CR-EOMCCSD(T),III method. Our calculations show that this black-box approximation is capable of providing results of CASPT2 or even near-MRCI quality over a wide range of nuclear geometries for the very challenging $B\ ^1\Delta_g$ and $B'\ ^1\Sigma_g^+$ states of the C_2 molecule. Similar findings have been obtained earlier in studies of entire excited-state potential curves of the "easier" CH$^+$ and HF

molecules, and vertical and adiabatic excitations in ozone and other small systems,[28,58] but this is the first time when we have used the CR-EOMCCSD(T) methodology to examine larger portions of excited-state potentials involving extremely large configurational quasidegeneracy effects, which can normally only be handled by sophisticated multireference approaches.

The problem that will have to be addressed in the future is that the CR-CCSD(T),III/CR-EOMCCSD(T),III calculations bring the nearly degenerate $X\,{}^1\Sigma_g^+$ and $B'\,{}^1\Sigma_g^+$ states too close to each other, so that they become virtually degenerate. Careful examination of the avoided crossing region suggests that the CR-CCSD(T),III/CR-EOMCCSD(T),III method makes the $X\,{}^1\Sigma_g^+$ and $B'\,{}^1\Sigma_g^+$ states degenerate at $R \approx 1.69$ Å; at $R=1.69$ Å, the energy gap between the $X\,{}^1\Sigma_g^+$ and $B'\,{}^1\Sigma_g^+$ states resulting from the CR-CCSD(T),III/CR-EOMCCSD(T),III calculations is only 0.1 kcal mol^{-1}. This problem is indicative of the difficulties that all noniterative single-reference CC/EOMCC methods, using elements of perturbation theory to estimate higher-order effects, have with the avoided crossings involving states of the same symmetry (cf. Ref. 122 for a discussion). In fact, this problem is not uncommon to high-level MRCI methods, which have difficulties with describing avoided crossings with small energy gaps once the Davidson corrections are added to MRCI energies. The genuine multireference methods or the iterative multireference-like EOMCC approximations, such as the active-space EOMCCSDt approach,[53–55] combined with appropriate orbital optimization techniques (such as CASSCF) may be the only practical approaches that can handle very small energy gaps between states of the same symmetry, while providing accurate results in other regions of potential energy surfaces. It is also possible that the combination of the CR-CCSD(T),III/CR-EOMCCSD(T),III method with suitable orbital optimization techniques may alleviate the problem of describing the small energy gap between the $X\,{}^1\Sigma_g^+$ and $B'\,{}^1\Sigma_g^+$ states observed in our calculations, but we are unable to perform such computations at this time. We have, however, examined the behavior of different variants of the CR-CCSD(T)/CR-EOMCCSD(T) theory proposed in Refs. 28 and 58 in the vicinity of the avoided crossing involving the $X\,{}^1\Sigma_g^+$ and $B'\,{}^1\Sigma_g^+$ states of C_2. Our analysis indicates that the most complete CR-CCSD(T),III/CR-EOMCCSD(T),III and CR-CCSD(T),ID/CR-EOMCCSD(T),ID approaches, which are also the overall most accurate CR-CCSD(T)/CR-EOMCCSD(T) approximations, behave in a very similar way, bringing the $X\,{}^1\Sigma_g^+$ and $B'\,{}^1\Sigma_g^+$ states too close to each other, as described above. In these two methods, the perturbative triples amplitudes defining the approximate forms of the three-body components of the cluster operator T and linear excitation operator R_K, which are used to determine the noniterative triples corrections to CCSD/EOMCCSD energies, are calculated using the diagonal elements of the triples-triples block of the matrix representing the Hamiltonian H or the EOMCCSD similarity-transformed Hamiltonian $\bar{H}$.[28,58] These diagonal matrix elements, $\langle\Phi_{ijk}^{abc}|H|\Phi_{ijk}^{abc}\rangle$ or $\langle\Phi_{ijk}^{abc}|\bar{H}|\Phi_{ijk}^{abc}\rangle$, respectively, are used in the CR-CCSD(T),III/CR-

EOMCCSD(T),III and CR-CCSD(T),ID/CR-EOMCCSD(T),ID methods, instead of the more usual perturbation theory denominators $(\varepsilon_a+\varepsilon_b+\varepsilon_c-\varepsilon_i-\varepsilon_j-\varepsilon_k)$ defined in terms of orbital energy differences, to improve the accuracy of the CR-EOMCCSD(T) results for excited states.[58] If we replace the diagonal matrix elements $\langle\Phi_{ijk}^{abc}|H|\Phi_{ijk}^{abc}\rangle$ or $\langle\Phi_{ijk}^{abc}|\bar{H}|\Phi_{ijk}^{abc}\rangle$ in the CR-CCSD(T)/CR-EOMCCSD(T) energy expressions by the orbital energy differences $(\varepsilon_a+\varepsilon_b+\varepsilon_c-\varepsilon_i-\varepsilon_j-\varepsilon_k)$, as is done in variants IA and IIA of the CR-CCSD(T)/CR-EOMCCSD(T) theory[28,58] [also, in the original ground-state CR-CCSD(T) approach[18,19]], the avoided crossing involving the $X\,{}^1\Sigma_g^+$ and $B'\,{}^1\Sigma_g^+$ states is described much better than in the CR-CCSD(T),III/CR-EOMCCSD(T),III and CR-CCSD(T),ID/CR-EOMCCSD(T),ID cases, although none of the CR-CCSD(T)/CR-EOMCCSD(T) methods can provide a good description of the asymptotic region. This is illustrated in Fig. 8, using the CR-CCSD(T),IIA/CR-EOMCCSD(T),IIA results as an example. As shown in Fig. 8(a), the problem of the unphysical degeneracy of the $X\,{}^1\Sigma_g^+$ and $B'\,{}^1\Sigma_g^+$ states at $R \approx 1.69$ Å and the resulting nonsmooth behavior of the corresponding potential energy curves created by the CR-CCSD(T),III/CR-EOMCCSD(T),III method is eliminated by the CR-CCSD(T),IIA/CR-EOMCCSD(T),IIA approximation. According to the CR-CCSD(T),IIA/CR-EOMCCSD(T),IIA calculations, the closest approach of the $X\,{}^1\Sigma_g^+$ and $B'\,{}^1\Sigma_g^+$ potentials occurs at $R \approx 2.0$ Å, where both states are separated by 13 kcal mol^{-1}, in reasonable agreement with $\sim$10 kcal mol^{-1} obtained wth full CI. The problem is that the overall accuracy of the CR-CCSD(T),IIA/CR-EOMCCSD(T),IIA results, including errors relative to full CI and NPE values, is not as high as the accuracy of the CR-CCSD(T),III/CR-EOMCCSD(T),III results [cf. Figs. 6(b) and 8(b) and Table IV], although all variants of the CR-CCSD(T)/CR-EOMCCSD(T) theory provide considerable improvements in the poor EOMCCSD results. In particular, the $B\,{}^1\Delta_g$ curve resulting from the CR-EOMCCSD(T),IIA calculations lies somewhat too high and does not cross the corresponding $X\,{}^1\Sigma_g^+$ curve, as it should do according to the CR-CCSD(T),III/CR-EOMCCSD(T),III and full CI calculations. Thus, the simplified CR-CCSD(T)/CR-EOMCCSD(T) methods, such as CR-CCSD(T),IIA/CR-EOMCCSD(T),IIA, which use the orbital energy differences $(\varepsilon_a+\varepsilon_b+\varepsilon_c-\varepsilon_i-\varepsilon_j-\varepsilon_k)$ rather than the diagonal matrix elements $\langle\Phi_{ijk}^{abc}|H|\Phi_{ijk}^{abc}\rangle$ or $\langle\Phi_{ijk}^{abc}|\bar{H}|\Phi_{ijk}^{abc}\rangle$ to define the perturbation theory denominators for triples energy corrections, provide a smooth and reasonably accurate description of the avoided crossing involving the $X\,{}^1\Sigma_g^+$ and $B'\,{}^1\Sigma_g^+$ states, and significant improvements in the results relative to the underlying EOMCCSD approach, but this is done at the expense of loosing the high accuracy observed in the CR-CCSD(T),III/CR-EOMCCSD(T),III calculations. The above analysis indicates that it may be possible to obtain an accurate description of the challenging avoided crossings involving states of the same symmetry, including the avoided crossing of the $X\,{}^1\Sigma_g^+$ and $B'\,{}^1\Sigma_g^+$ states of C_2, with the CR-CCSD(T)/CR-EOMCCSD(T) methodology if we choose the right form of the perturbation theory denominators that enter the CR-
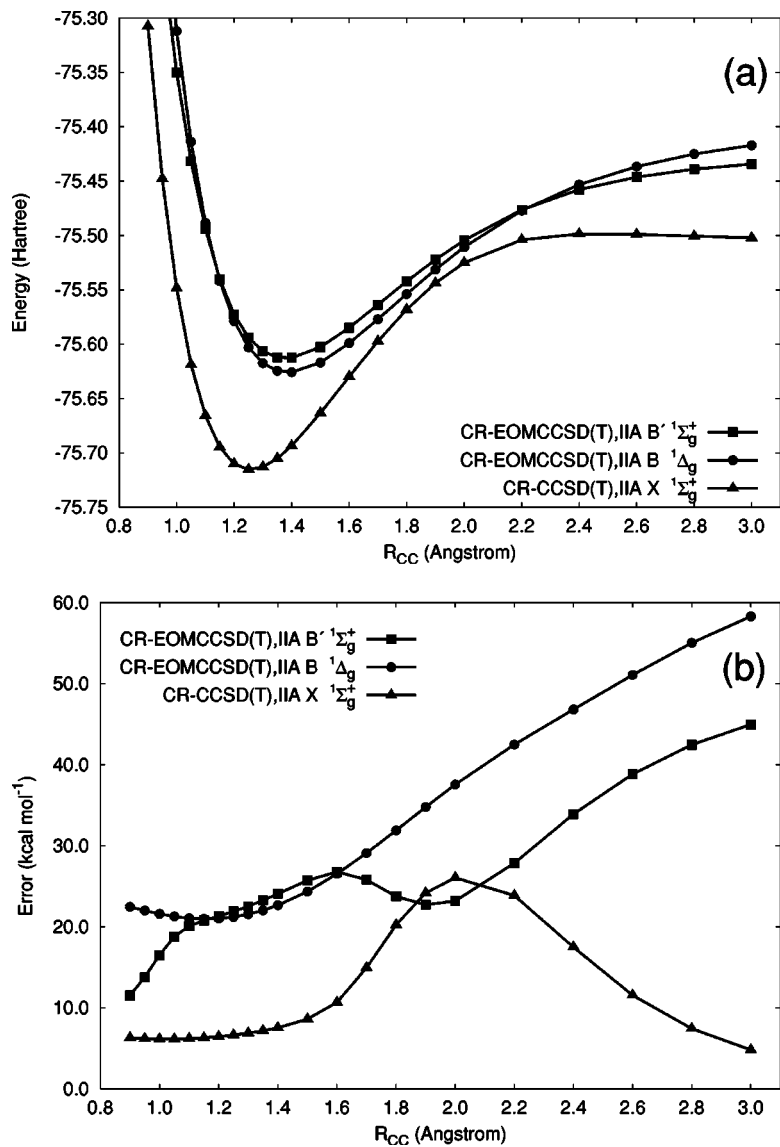
FIG. 8. Results of the CR-CCSD(T),IIA/CR-EOMCCSD(T),IIA calculations for the $X\,^1\Sigma_g^+$, $B\,^1\Delta_g$, and $B'\,^1\Sigma_g^+$ states of C_2: (a) potential energy curves, (b) errors relative to full CI.

CCSD(T)/CR-EOMCCSD(T) triples corrections, but one has to develop better schemes than CR-CCSD(T),IIA/CR-EOMCCSD(T),IIA in order to match the high accuracy obtained with the CR-CCSD(T),III/CR-EOMCCSD(T),III approximation. As the results for the $X\,^1\Sigma_g^+$ and $B\,^1\Delta_g$ states indicate, the CR-CCSD(T),III/CR-EOMCCSD(T),III method has no problem with describing the curve crossings involving states of different symmetries and, in fact, we have preliminary numerical evidence (using the low-lying states of ammonia as an example) showing that the CR-CCSD(T)/CR-EOMCCSD(T) methods of Ref. 58 have no difficulty with describing the avoided crossings that emerge from the true curve crossings as a result of symmetry lowering.[123]

IV. CONCLUSIONS

A previous study[3] has shown that the $X\,^1\Sigma_g^+$, $B\,^1\Delta_g$, and $B'\,^1\Sigma_g^+$ states of C_2 are tremendously challenging for single-reference electronic structure methods, even those incorporating very extensive treatments of electron correlation such as UHF CCSD(T) or CISDTQ. This difficulty is due to the presence of near degeneracies among the electron configura-

tions all along the potential curves. Here we have examined the reliability of two types of theoretical approaches which are designed to improve the results in such situations: multireference methods and single-reference completely renormalized CC/EOMCC theories.

Multireference computations were based on CASSCF reference functions, which provide qualitatively correct descriptions of the three potential curves. When the CASSCF reference is improved via MRPT or MRCI techniques, the potential curves accurately mimic the exact full CI results. The CASPT2 version of MRPT demonstrated NPEs of $3-4$ kcal mol^{-1}, which are similar[65,66] to those for bond-breaking reactions in BH, CH_4, HF, H_2O, and N_2. Very extensive MRCI wave functions yielded even smaller NPEs of $0.4-0.7$ kcal mol^{-1}, which is again comparable to the NPEs observed in other systems when the active space is well-chosen.[65,66] This demonstrates that the CASPT2 and MRCI methods are robust even to the curve crossings and severe near degeneracies encountered in C_2.

A more black-box approach, employing the single-reference CR-CC/CR-EOMCC methodology, was also applied to C_2 to assess its performance compared to the more

intricate (and harder to use) multireference methods. This represents the first application of these methods to a challenging situation involving curve crossings among ground- and excited-state potential energy curves of a multiply bonded system. The CR-CCSD(T)/CR-EOMCCSD(T) approach dramatically improves upon the underlying CCSD/EOMCCSD potentials, which do not have the correct qualitative relationships with one another. However, it remains a single-reference theory, and it ultimately has difficulty near the dissociation limit. On the other hand, for all internuclear separations R from the $R=1.1-1.8$ Å region, the quality of the CR-CCSD(T)/CR-EOMCCSD(T) potentials approaches that of CASPT2 or MRCI, particularly for the excited states; the NPEs characterizing the CR-CCSD(T)/CR-EOMCCSD(T) results in this region are 8.3, 1.3, and 2.1 kcal mol^{-1} for the $X\,^1\Sigma_g^+$, $B\,^1\Delta_g$, and $B'\,^1\Sigma_g^+$ states, respectively. This demonstrates that, for a wide range of geometries, the relatively simple noniterative CR-CC/CR-EOMCC approximations can be a reasonable alternative to the more sophisticated multireference methods even for a very difficult system such as the C_2 molecule.

ACKNOWLEDGMENTS

[1] G. Herzberg, *Spectra of Diatomic Molecules*, Molecular Spectra and Molecular Structure Vol. 1 (Krieger, Malabar, FL, 1991).

[2] K. P. Huber and G. Herzberg, *Constants of Diatomic Molecules* (Van Nostrand Reinhold, New York, 1979).

[3] M. L. Abrams and C. D. Sherrill, J. Chem. Phys. **121**, 9211 (2004).

[4] W. D. Laidig, P. Saxe, and R. J. Bartlett, J. Chem. Phys. **86**, 887 (1987).

[5] J. Čížek, J. Chem. Phys. **45**, 4256 (1966).

[6] G. D. Purvis III and R. J. Bartlett, J. Chem. Phys. **76**, 1910 (1982).

[7] G. E. Scuseria, A. C. Scheiner, T. J. Lee, J. E. Rice, and H. F. Schaefer III, J. Chem. Phys. **86**, 2881 (1987).

[8] G. E. Scuseria, C. L. Janssen, and H. F. Schaefer III, J. Chem. Phys. **89**, 7382 (1988).

[9] T. J. Lee and J. E. Rice, Chem. Phys. Lett. **150**, 406 (1988).

[10] P. Piecuch and J. Paldus, Int. J. Quantum Chem. **36**, 429 (1989).

[11] M. Urban, J. Noga, S. J. Cole, and R. J. Bartlett, J. Chem. Phys. **83**, 4041 (1985).

[12] P. Piecuch and J. Paldus, Theor. Chim. Acta **78**, 65 (1990).

[13] K. Raghavachari, G. W. Trucks, J. A. Pople, and M. Head-Gordon, Chem. Phys. Lett. **157**, 479 (1989).

[14] K. B. Ghose, P. Piecuch, and L. Adamowicz, J. Chem. Phys. **103**, 9331 (1995).

[15] P. Piecuch, V. Špirko, A. E. Kondo, and J. Paldus, J. Chem. Phys. **104**, 4699 (1996).

[16] P. Piecuch, S. A. Kucharski, and R. J. Bartlett, J. Chem. Phys. **110**, 6103 (1999).

[17] P. Piecuch, S. A. Kucharski, and V. Špirko, J. Chem. Phys. **111**, 6679 (1999).

[18] P. Piecuch and K. Kowalski, in *Computational Chemistry: Reviews of Current Trends*, edited by J. Leszczyński (World Scientific, Singapore, 2000), Vol. 5, pp. 1–104.

[19] K. Kowalski and P. Piecuch, J. Chem. Phys. **113**, 18 (2000).

[20] K. Kowalski and P. Piecuch, J. Chem. Phys. **113**, 5644 (2000).

[21] K. Kowalski and P. Piecuch, Chem. Phys. Lett. **344**, 165 (2001).

[22] P. Piecuch, S. A. Kucharski, and K. Kowalski, Chem. Phys. Lett. **344**, 176 (2001).

[23] P. Piecuch, S. A. Kucharski, V. Špirko, and K. Kowalski, J. Chem. Phys. **115**, 5796 (2001).

[24] P. Piecuch, K. Kowalski, I. S. O. Pimienta, and S. A. Kucharski, in *Low-Lying Potential Energy Surfaces*, ACS Symposium Series Vol. 828, edited by M. R. Hoffmann and K. G. Dyall (American Chemical Society, Washington, D. C., 2002), pp. 31–64.

[25] P. Piecuch, K. Kowalski, I. S. O. Pimienta, and M. J. McGuire, Int. Rev. Phys. Chem. **21**, 527 (2002).

[26] M. J. McGuire, K. Kowalski, and P. Piecuch, J. Chem. Phys. **117**, 3617 (2002).

[27] P. Piecuch, K. Kowalski, P.-D. Fan, and I. S. O. Pimienta, in *Advanced Topics in Theoretical Chemical Physics*, Progress in Theoretical Chemistry and Physics, Vol. 12, edited by J. Maruani, R. Lefebvre, and E. Brändas (Kluwer, Dordrecht, 2003), pp. 119–206.

[28] P. Piecuch, K. Kowalski, I. S. O. Pimienta *et al.*, Theor. Chem. Acc. **112**, 349 (2004).

[29] M. J. McGuire, P. Piecuch, K. Kowalski, S. A. Kucharski, and M. Musiał, J. Phys. Chem. A **108**, 8878 (2004).

[30] A. Dutta and C. D. Sherrill, J. Chem. Phys. **118**, 1610 (2003).

[31] J. Noga and R. J. Bartlett, J. Chem. Phys. **86**, 7041 (1987); **89**, 3401(E) (1988).

[32] G. E. Scuseria and H. F. Schaefer III, Chem. Phys. Lett. **152**, 382 (1988).

[33] S. A. Kucharski and R. J. Bartlett, J. Chem. Phys. **108**, 9221 (1998).

[34] H. Monkhorst, Int. J. Quantum Chem., Quantum Chem. Symp. **11**, 421 (1977).

[35] H. Sekino and R. J. Bartlett, Int. J. Quantum Chem., Quantum Chem. Symp. **18**, 255 (1984).

[36] E. Daalgard and H. Monkhorst, Phys. Rev. A **28**, 1217 (1983).

[37] M. Takahashi and J. Paldus, J. Chem. Phys. **85**, 1486 (1986).

[38] H. Koch and P. Jørgensen, J. Chem. Phys. **93**, 3333 (1990).

[39] H. Koch, H. J. Aa. Jensen, P. Jørgensen, and T. Helgaker, J. Chem. Phys. **93**, 3345 (1990).

[40] J. Geertsen, M. Rittby, and R. J. Bartlett, Chem. Phys. Lett. **164**, 57 (1989).

[41] D. C. Comeau and R. J. Bartlett, Chem. Phys. Lett. **207**, 414 (1993).

[42] J. F. Stanton and R. J. Bartlett, J. Chem. Phys. **98**, 7029 (1993).

[43] P. Piecuch and R. J. Bartlett, Adv. Quantum Chem. **34**, 295 (1999).

[44] J. D. Watts and R. J. Bartlett, Chem. Phys. Lett. **233**, 81 (1995).

[45] J. D. Watts and R. J. Bartlett, Chem. Phys. Lett. **258**, 581 (1996).

[46] H. Koch, O. Christiansen, P. Jørgensen, and J. Olsen, Chem. Phys. Lett. **244**, 75 (1995).

[47] O. Christiansen, H. Koch, and P. Jørgensen, J. Chem. Phys. **103**, 7429 (1995).

[48] O. Christiansen, H. Koch, and P. Jørgensen, J. Chem. Phys. **105**, 1451 (1996).

[49] O. Christiansen, H. Koch, P. Jørgensen, and J. Olsen, Chem. Phys. Lett. **256**, 185 (1996).

[50] J. D. Watts and R. J. Bartlett, J. Chem. Phys. **101**, 3073 (1994).

[51] H. Larsen, J. Olsen, P. Jørgensen, and O. Christiansen, J. Chem. Phys. **113**, 6677 (2000); **114**, 10985(E) (2001).

[52] K. Hald, P. Jørgensen, J. Olsen, and M. Jaszuński, J. Chem. Phys. **115**, 671 (2001).

[53] K. Kowalski and P. Piecuch, J. Chem. Phys. **113**, 8490 (2000).

[54] K. Kowalski and P. Piecuch, J. Chem. Phys. **115**, 643 (2001).

[55] K. Kowalski and P. Piecuch, Chem. Phys. Lett. **347**, 237 (2001).

[56] K. Kowalski and P. Piecuch, J. Chem. Phys. **115**, 2966 (2001).

[57] K. Kowalski and P. Piecuch, J. Chem. Phys. **116**, 7411 (2002).

[58] K. Kowalski and P. Piecuch, J. Chem. Phys. **120**, 1715 (2004).

[59] A. I. Krylov, C. D. Sherrill, and M. Head-Gordon, J. Chem. Phys. **113**, 6509 (2000).

[60] S. A. Kucharski, M. Włoch, M. Musiał, and R. J. Bartlett, J. Chem. Phys. **115**, 8263 (2001).

[61] S. Hirata, J. Chem. Phys. **121**, 51 (2004).

[62] J. D. Watts and R. J. Bartlett, Int. J. Quantum Chem., Quantum Chem. Symp. **27**, 51 (1993).

[63] F. Jensen, Chem. Phys. Lett. **169**, 519 (1990).

[64] P. G. Szalay, J. Vazquez, C. Simmons, and J. F. Stanton, J. Chem. Phys. **121**, 7624 (2004).

[65] M. L. Abrams and C. D. Sherrill, J. Phys. Chem. A **107**, 5611 (2003).

[66] J. S. Sears and C. D. Sherrill, Mol. Phys. (in press).
[67] B. O. Roos, P. Linse, P. E. M. Siegbahn, and M. R. A. Blomberg, Chem. Phys. **66**, 197 (1982).
[68] K. Andersson, P.-Å. Malmqvist, B. O. Roos, A. J. Sadlej, and K. Woliński, J. Phys. Chem. **94**, 5483 (1990).
[69] K. Andersson, P.-Å. Malmqvist, and B. O. Roos, J. Chem. Phys. **96**, 1218 (1992).
[70] K. Andersson and B. O. Roos, in *Modern Electronic Structure Theory*, Advanced Series in Physical Chemistry Vol. 2, edited by D. R. Yarkony (World Scientific, Singapore, 1995), pp. 55–109.
[71] K. Woliński, H. L. Sellers, and P. Pulay, Chem. Phys. Lett. **140**, 225 (1987).
[72] K. Woliński and P. Pulay, J. Chem. Phys. **90**, 3647 (1989).
[73] K. Woliński, Theor. Chim. Acta **82**, 459 (1992).
[74] K. Hirao, Int. J. Quantum Chem., Quantum Chem. Symp. **26**, 517 (1992).
[75] K. Hirao, Chem. Phys. Lett. **190**, 374 (1992).
[76] K. Hirao, Chem. Phys. Lett. **196**, 397 (1992).
[77] P. M. Kozłowski and E. R. Davidson, J. Chem. Phys. **100**, 3672 (1994).
[78] P. M. Kozłowski and E. R. Davidson, Chem. Phys. Lett. **222**, 615 (1994).
[79] H. Nakano, J. Chem. Phys. **99**, 7983 (1993).
[80] M. W. Schmidt and M. S. Gordon, Annu. Rev. Phys. Chem. **49**, 233 (1998).
[81] I. Özkan, A. Kinal, and M. Balci, J. Phys. Chem. A **108**, 507 (2004).
[82] M. J. McGuire and P. Piecuch, J. Am. Chem. Soc. **127**, 2608 (2005).
[83] A. Kinal and P. Piecuch (unpublished).
[84] A. I. Krylov, Chem. Phys. Lett. **338**, 375 (2001).
[85] A. I. Krylov and C. D. Sherrill, J. Chem. Phys. **116**, 3194 (2002).
[86] L. V. Slipchenko and A. I. Krylov, J. Chem. Phys. **117**, 4694 (2002).
[87] Y. H. Shao, M. Head-Gordon, and A. I. Krylov, J. Chem. Phys. **118**, 4807 (2003).
[88] J. S. Sears, C. D. Sherrill, and A. I. Krylov, J. Chem. Phys. **118**, 9084 (2003).
[89] M. Tobita, S. A. Perera, M. Musial, R. J. Bartlett, M. Nooijen, and J. S. Lee, J. Chem. Phys. **119**, 10713 (2003).
[90] T. D. Crawford and J. F. Stanton, Int. J. Quantum Chem. **70**, 601 (1998).
[91] S. R. Gwaltney and M. Head-Gordon, Chem. Phys. Lett. **323**, 21 (2000).
[92] S. R. Gwaltney, C. D. Sherrill, and M. Head-Gordon, J. Chem. Phys. **113**, 3548 (2000).
[93] S. R. Gwaltney and M. Head-Gordon, J. Chem. Phys. **115**, 2014 (2001).
[94] S. Hirata, P.-D. Fan, A. A. Auer, M. Nooijen, and P. Piecuch, J. Chem. Phys. **121**, 12197 (2004).
[95] X. Li and J. Paldus, J. Chem. Phys. **107**, 6257 (1997).
[96] X. Li and J. Paldus, J. Chem. Phys. **108**, 637 (1998).
[97] X. Li and J. Paldus, Chem. Phys. Lett. **286**, 145 (1998).
[98] N. Oliphant and L. Adamowicz, J. Chem. Phys. **94**, 1229 (1991).
[99] P. Piecuch, N. Oliphant, and L. Adamowicz, J. Chem. Phys. **99**, 1875 (1993).
[100] P. Piecuch and L. Adamowicz, J. Chem. Phys. **100**, 5792 (1994).
[101] L. Adamowicz, P. Piecuch, and K. B. Ghose, Mol. Phys. **94**, 225 (1998).
[102] C. W. Bauschlicher and S. R. Langhoff, J. Chem. Phys. **87**, 2919 (1987).
[103] M. L. Leininger, C. D. Sherrill, W. D. Allen, and H. F. Schaefer, J. Chem. Phys. **108**, 6717 (1998).
[104] M. L. Abrams and C. D. Sherrill, J. Chem. Phys. **118**, 1604 (2003).
[105] M. Boggio-Pasqua, A. I. Voronin, P. Halvick, and J.-C. Rayez, J. Mol. Struct.: THEOCHEM **531**, 159 (2000).
[106] B. O. Roos, P. R. Taylor, and P. E. M. Siegbahn, Chem. Phys. **48**, 157 (1980).
[107] K. K. Docken and J. Hinze, J. Chem. Phys. **57**, 4928 (1972).
[108] K. Ruedenberg, L. M. Cheung, and S. T. Elbert, Int. J. Quantum Chem. **16**, 1069 (1979).
[109] C. D. Sherrill and H. F. Schaefer, Adv. Quantum Chem. **34**, 143 (1999).
[110] T. D. Crawford, C. D. Sherrill, E. F. Valeev *et al.*, J. Comput. Chem. (submitted).
[111] P. Celani and H.-J. Werner, J. Chem. Phys. **112**, 5546 (2000).
[112] H.-J. Werner, P. J. Knowles, M. Schütz *et al.*, MOLPRO, a package of *ab initio* programs designed by H.-J. Werner and P. J. Knowles, Version 2002.6, see http://www.molpro.net
[113] P. Piecuch, S. A. Kucharski, K. Kowalski, and M. Musiał, Comput. Phys. Commun. **149**, 71 (2002).
[114] K. Kowalski, M. Włoch, P. Piecuch, S. A. Kucharski, M. Musiał, and M. W. Schmidt (unpublished).
[115] M. W. Schmidt, K. K. Baldridge, J. A. Boatz *et al.*, J. Comput. Chem. **14**, 1347 (1993).
[116] J. F. Stanton, J. Gauss, J. D. Watts, W. J. Lauderdale, and R. J. Bartlett, Int. J. Quantum Chem., Quantum Chem. Symp. **26**, 879 (1992).
[117] P. E. M. Siegbahn, Int. J. Quantum Chem. **18**, 1229 (1980).
[118] P. Saxe, Y. Yamaguchi, and H. F. Schaefer, J. Chem. Phys. **77**, 5647 (1982).
[119] R. S. Grev and H. F. Schaefer, J. Chem. Phys. **96**, 6850 (1992).
[120] C. D. Sherrill and H. F. Schaefer, J. Phys. Chem. **100**, 6069 (1996).
[121] B. O. Roos, K. Andersson, M. P. Fülscher, P.-Å. Malmqvist, L. Serrano-Andrés, K. Pierloot, and M. Merchán, Adv. Chem. Phys. **93**, 219 (1996).
[122] J. F. Stanton, J. Chem. Phys. **115**, 10382 (2001).
[123] A. W. Jasper, S. Nangia, C. Zhu, D. G. Truhlar, M. J. McGuire, and P. Piecuch (unpublished).